Least Squares Estimation of Range by Phase Unwrapping

Assad Akhlaq

MSc. Electrical Eng.

BSc. Electrical Eng.

Thesis submitted for the degree of
Doctor of Philosophy
in
Telecommunications

University of
South Australia

Institute for
Telecommunications
Research

January 15, 2016

Contents

List of Figures

List of Tables

Summary

Publications

Declaration

Acknowledgements

Chapter 1

Introduction

1.1 Introduction

In numerous signal processing applications, such as speech, magnetic resonance imaging (MRI) and radar imaging devices such as synthetic aperture radar (SAR), a quantity of primary interest is the phase of a received signal. For example, in radar applications, the phase may provide information about the distance to a target. An inherent property of the phase is that only its principal component is observed, that is, the observed value of the phase is always in the range $[-\pi, \pi)$. In applications, this leads to ambiguities in the value of some parameter of interest (such as the distance to a target). The task of rectifying these ambiguities is called *phase unwrapping*. In this thesis we consider the problem of range or distance estimation and pioneer a novel approach to phase unwrapping that is based on a fundamental task in algebraic number theory, called lattice reduction. This new approach promises to be both computationally simple, and statistically more accurate and robust than the current state-of-the-art phase unwrapping algorithms.

Range (or distance) estimation is an important component in modern technologies such as electronic surveying [1, 2], global positioning [3, 4], and ranging cameras [5, 6]. Common methods of range estimation are based upon received signal strength [7, 8], time of flight (or time of arrival) [9, 10], and phase of arrival [11, 12]. Phase of arrival has become the technique of choice in modern high precision surveying, global positioning,

and ranging cameras [5, 6, 13–16] because it provides the most accurate range estimates in many applications.

A difficulty with phase of arrival is that only the principal component of the phase can be observed. This limits the range that can be unambiguously estimated, that is, the observed value of the phase is always in the range $[-\pi, \pi)$. This is sometimes referred to as the problem of *phase ambiguity* and it is related to what has been called the *notorious wrapping problem* in the circular statistics and meteorology literature [17]. One approach to address this problem is to utilise signals of multiple different wavelengths and observe the phase at each. The range can then be measured within an interval of length equal to the least common multiple of the wavelengths. Range estimators from such observations have been studied by numerous authors. Techniques include the beat wavelength method of Towers et al. [18, 19], the method of excess fractions [20–23], and methods based on the Chinese Remainder Theorem (CRT) [24–31]. Least squares/maximum likelihood and maximum a posteriori (MAP) estimators of range have been studied by Teunissen [4], Hassibi and Boyd [32], and more recently by Li et al. [33] and Akhlaq et al. [34].

This thesis focuses on the least squares estimation of range. A key realisation is that the least squares estimator can be efficiently computed by solving a well known integer programming problem, that of computing a *closest point* in a *lattice* [35]. Teunissen [4] appears to have been the first to have realised this connection. Efficient general purpose algorithms for computing a closest lattice point require a *basis* for the lattice. Constructing a basis for the least squares estimator of range is non-trivial. Based upon the work of Teunissen [4], and under some assumptions about the distribution of phase errors, Hassibi and Boyd [32] constructed a basis for the MAP estimator. Their construction does not apply for the least squares estimator.[1] This is problematic because the MAP estimator requires sufficiently accurate prior knowledge of the range, whereas the least squares estimator is accurate without this knowledge.

[1] The least squares estimator is also the maximum likelihood estimator under the assumptions made by Hassibi and Boyd [32]. The matrix G in [32] is rank deficient in the least squares and weighted least squares cases and so G is not a valid lattice basis. In particular, observe that the determinant of G [32, p. 2948] goes to zero as the a priori assumed variance σ_x^2 goes to infinity.

An explicit basis construction for the least squares estimator was recently given by Li et. al. [33] under the assumption that the wavelengths can be scaled to pairwise relatively prime integers. This assumption is impractical because it forces to use only the wavelengths that can be scaled to pairwise relatively prime integers. This effects the accuracy of the range estimator because the accuracy of the range estimator depends upon the wavelengths. It is possible that the wavelengths that give the most accurate range estimates could not be scaled to pairwise relatively prime integers. The dependence of estimation accuracy upon the measurement wavelengths leads to two important questions:

- Whether it is possible to devise a general basis construction method for the least squares estimator that is independent of mutually co-prime restriction on the scaled wavelengths?
- Given a general basis construction method, whether it is possible to select wavelengths that maximise the accuracy of the least squares range estimator?

The first question is addressed in this thesis by employing some important properties from lattice theory. Solution to the first question naturally leads to the second important question of selecting wavelengths. However, the relationship between measurement wavelengths and range estimation accuracy is nontrivial and this complicates wavelength selection procedures. The selection procedure is typically subject to practical constraints such minimum and maximum wavelength (i.e. bandwidth constraints) and constraints on the maximum identifiable range. Procedures for wavelength selection have been described for the beat wavelength method [18] and for the method of excess fractions [21]. Some of these methods are heuristic and require a non-negligible amount of experimentation. however, procedures for selecting wavelengths for the CRT and least squares range estimators have not yet been developed. The second question of selecting wavelengths that maximise the estimation accuracy is addressed in the last part of the thesis.

1.2 Thesis Outline and Contributions

Estimation of range (or distance) using phase of arrival based method has extensively been studied in the literature using the beat wavelength method [18, 19], the method of excess fractions [20–23], methods based on the Chinese Remainder Theorem (CRT) [24–31], and the least squares/maximum likelihood and maximum a posteriori (MAP) estimators [4, 32, 33]. Each of these methods have some limitations when applied to practical systems. This thesis aims to provide a practically applicable solution to the least squares estimation of range based on the phase of arrival method. A brief overview of the major contributions of each chapter is presented in the following.

Chapter 2 — Background Overview

This chapter presents a brief overview of concepts and background literature required for the understanding of the thesis. Section I introduces some introductory concepts from lattice theory. The main focus of this section is on the Voronoi cell, the nearest lattice point problem, dual lattices, and the properties of lattices generated by intersection with or projection onto a subspace. These will be the most useful concepts used for the basis construction, robustness bound, and the wavelength selection method for the least squares range estimator described in Chapters 3, 4 and 5. Section II introduces the range estimation problem from multiple phase observations and provides an overview of the existing range estimation techniques such as the beat wavelength method, the method of excess fractions, and the CRT method. In Section III we provide an overview of wavelength selection algorithms available in the literature for phase of arrival based range estimators.

Chapter 3 — Basis Construction for Range Estimation by Phase Unwrapping

In this chapter we first introduce the system model used for the phase of arrival based range estimator that will be used throughout the thesis. We then derive the least

squares estimator of the range using multiple phase observation at multiple frequencies. We show that how the solution to the least squares range estimator can be obtained by solving a problem from computational number theory called the closest lattice point problem. Finding a closest point in a lattice requires a basis for the lattice. Constructing a basis is non-trivial and an explicit construction has only been given in the case that the wavelengths can be scaled to pairwise relatively prime integers. In this chapter we present an explicit construction of a basis without this assumption on the wavelengths. This is important because the accuracy of the range estimator depends upon the wavelengths. The solution for the least squares range estimator provided in this chapter leads us to a natural question of how to select a set of wavelengths that results in highly accurate range estimates.

This chapter includes material published in the following journal paper:

- Assad Akhlaq, R. G. McKilliam, and R. Subramanian, "Basis Construction for Range Estimation by Phase Unwrapping," *IEEE Signal Processing Letters,* Vol. 22, No. 11, November 2015.

Chapter 4 — Robustness of the Least Square Range Estimator

The least squares range estimator makes an estimate of the so called integer *wrapping variables*. These wrapping variables are related to the whole number of wavelengths that occur over the range. Accurate estimators of the wrapping variables are also expected to be the accurate estimators of the range. This chapter derives an upper bound on the phase measurement errors such that if all absolute phase measurement errors are less than this bound, then the least squares range estimator is guaranteed to correctly estimate the wrapping variables and hence the range. This bound is derived using a lattice theory property called the *inradius*. It is noted that this bound depends upon the values of the wavelengths used for range estimation. This naturally leads to the question of whether it is possible to select wavelengths that maximise the inradius. This is an interesting and nontrivial problem that we address in Chapter 5.

This chapter includes material published in the following conference paper:

- Assad Akhlaq, R. G. McKilliam, and André Pollok, "Robustness of the Least Squares Range Estimator," in *Proc. Australian Communications Theory Workshop (AusCTW),* Melbourne, Australia, Jan 2016.

Chapter 5 — Selecting Wavelengths for Least Squares Range Estimation

Motivated from the results in Chapter 3 and Chapter 4, in this chapter we develop an algorithm to automatically select wavelengths for use with the least square range estimator. In this chapter a key realisation is made that discloses the nontrivial relationship between the measurement wavelengths and the range estimation accuracy by relating the measurement wavelengths to the determinant of the lattice. This observation is utilised to design an optimisation criterion that is connected with the mean square error of the least squares range estimator. For this purpose interesting properties of a particular class of *lattices* are used. These properties lead to a simple and sufficiently accurate approximation for the mean square range error in terms of the wavelengths. The resulting constrained optimisation problem is solved by a depth first search.

This chapter includes material submitted in the following journal paper:

- Assad Akhlaq, R. G. McKilliam, R. Subramanian and André Pollok, "Selecting Wavelengths for Least Squares Range Estimation," submitted to *IEEE Trans. Signal Processing,* Jan. 2016.

Chapter 6 — Conclusion and Future Work

This chapter briefly summarises the thesis contributions. The chapter concludes with a discussion on improving the frequency selection algorithm and provides future research directions related to the work presented in this thesis.

In essence, this thesis provides an important research contribution for practical realisation of an efficient least squares range estimator. The basis construction method for the least squares range estimator provided in Chapter 3 removes the restriction that the scaled wavelengths must be mutually co-prime integers. Chapter 4 provides an upper bound on phase measurement errors to guarantee the correct estimation of wrapping variables. The relaxation on the use of measurement wavelengths and identification of an upper bound on phase measurement errors in Chapters 3 and 4 pave the path towards the identification of an optimised set of wavelengths to increase the accuracy of the least squares range estimator. A simple depth first search algorithm is provided in Chapter 5 to select wavelengths that minimises the mean square error of the least squares range estimator. Chapter 6 concludes this thesis and provides future research directions.

Chapter 2

Background Overview

This thesis employs some important concepts from lattice theory to address the problem of the range (or distance) estimation. In this chapter we first introduce these important concepts from lattice theory and then describe some existing techniques used in the literature for range estimation. In this chapter we also discuss some existing wavelength selection methods devised for different range estimation techniques. This discussion will lay down the foundations for the remainder of the thesis. This chapter is structured as follows. In Section 2.1 we describe some introductory concepts from lattice theory that are required for better understanding of the rest of the thesis. Range (or distance) estimation problem is described in Section 2.2. Some important techniques for range estimation are discussed in Section 2.3. Section 2.4 presents wavelength selection strategies available in the literature for different range estimation techniques.

2.1 Lattice Theory

Historical foundations of this field were laid down by investigations of some famous mathematicians such as Gauss and Lagrange in the late 18th century and later by Minkowski. Lattices have now become a hot research topic due to its applications in wide range of problems such as cryptography and cryptanalysis, image processing, signal processing for MIMO communications, frequency estimation, and range estimation

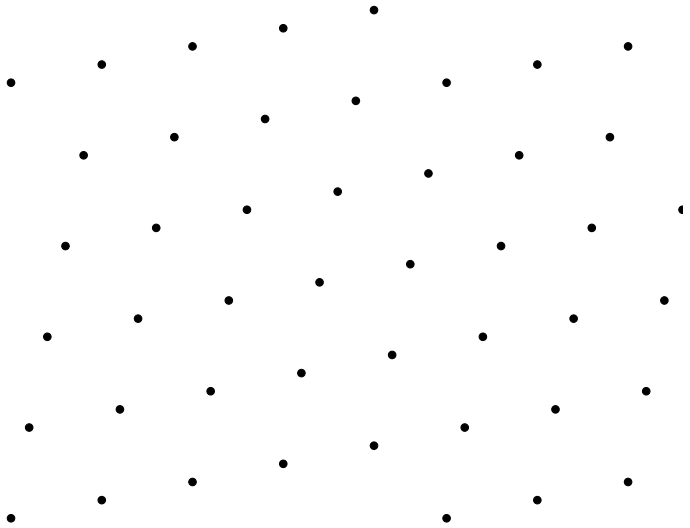

Figure 2.1: A lattice in $\mathbb{R}^2$.

etc. In the following we provide an overview of some important concepts from lattice theory.

A **lattice** is a set of points in n-dimensional Euclidean space. It has a periodic structure as shown in Figure 2.1. Let $\mathbf{b}_1, ..., \mathbf{b}_n$ be linearly independent vectors from m-dimensional Euclidean space $\mathbb{R}^m$ with $m \geq n$. The set of vectors

$$\Lambda = \{u_1\mathbf{b}_1 + \cdots + u_n\mathbf{b}_n \ ; \ u_1, \ldots, u_n \in \mathbb{Z}\}$$

is called an n-dimensional *lattice*. The elements of Λ are called *lattice points* or *lattice vectors*.

The vectors $\mathbf{b}_1, \ldots, \mathbf{b}_n$ form a **basis** for the lattice Λ. We can equivalently write

$$\Lambda = \{\mathbf{Bu} \ ; \ \mathbf{u} \in \mathbb{Z}^n\}$$

where $\mathbf{B}$ is the $m \times n$ matrix with columns $\mathbf{b}_1, \ldots, \mathbf{b}_n$. The matrix $\mathbf{B}$ is called a **basis** or **generator** for Λ. The basis of a lattice is not unique. If $\mathbf{U}$ is an $n \times n$ matrix with integer elements and determinant $\det \mathbf{U} = \pm 1$ then $\mathbf{U}$ is called a **unimodular matrix** and $\mathbf{B}$ and $\mathbf{BU}$ are both bases for Λ. When $m = n$ the lattice is said to be **full rank**. When $m > n$ the lattice points lie in the n-dimensional subspace of $\mathbb{R}^m$ spanned by

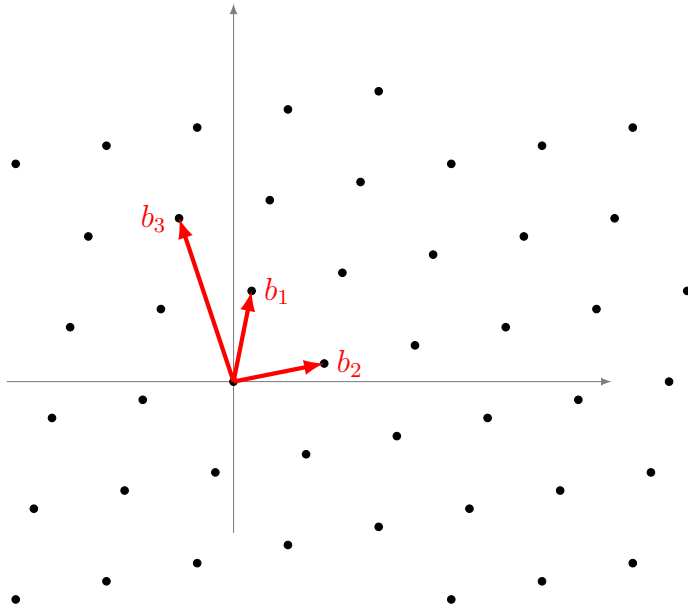

Figure 2.2: Two of the many possible basis matrices for a lattice in $\mathbb{R}^2$ are shown i.e. $\mathbf{B}_1 = [\mathbf{b}_1 \quad \mathbf{b}_2]$ and $\mathbf{B}_2 = [\mathbf{b}_1 \quad \mathbf{b}_3]$.

$\mathbf{b}_1, \ldots, \mathbf{b}_n$. The set of integers $\mathbb{Z}^n$ is called the **integer lattice** with the $n \times n$ identity matrix $\mathbf{I}$ as a basis.

The **span** of a lattice (Λ) is the linear space spanned by its vectors, that is,

$$\text{span}(\Lambda) = \text{span}(\mathbf{B}) = \{\mathbf{By} | \mathbf{y} \in \mathbb{R}^n\}$$

Let $\mathbf{B}$ be the basis of a lattice Λ then the matrix

$$\mathbf{A} = \mathbf{B}'\mathbf{B}$$

is called the **Gram matrix** and $\mathbf{B}'$ denotes the transpose of $\mathbf{B}$.

The parallelepiped formed by basis vectors $\mathbf{b}_1, \ldots, \mathbf{b}_n$ is called a **fundamental parallelepiped** of the lattice Λ. For a lattice with a basis $\mathbf{B}$ the fundamental parallelepiped $\mathcal{P}(B)$ is defined as

$$\mathcal{P}(B) = \{\mathbf{Bx} | \mathbf{x} \in \mathbb{R}^n, \forall i : 0 \leq x_i < 1\}$$

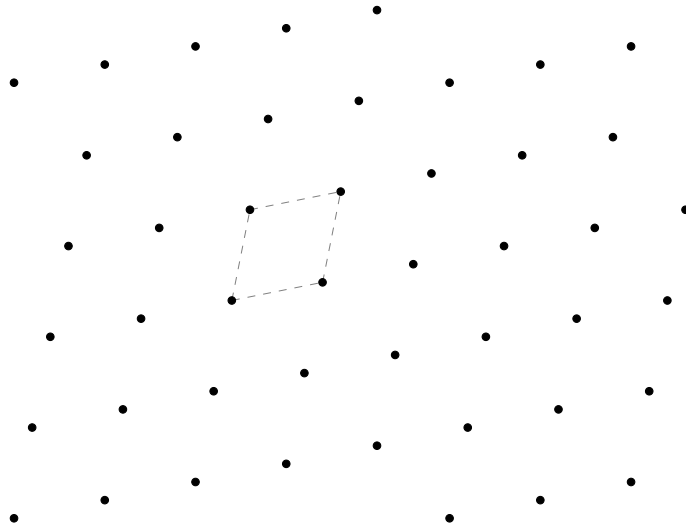

Figure 2.3: A lattice in $\mathbb{R}^2$.

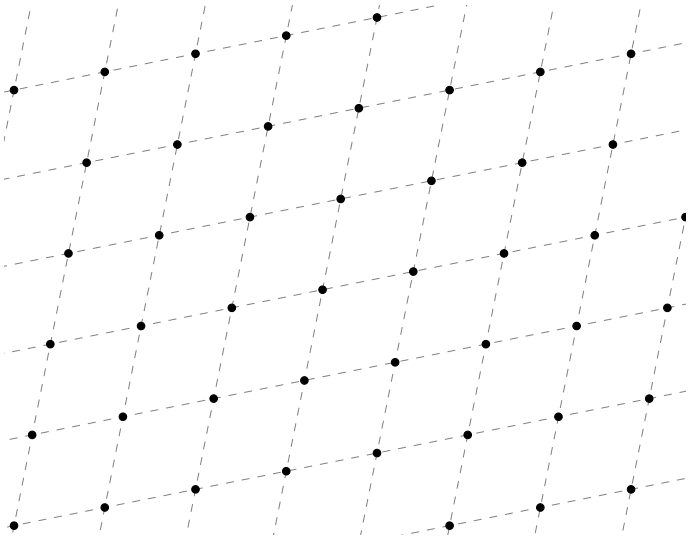

Figure 2.4: Tiling of the entire $span(\Lambda)$ by parallelepiped placed at each lattice point.

A fundamental parallelepiped has n-dimensional volume $\sqrt{\mathbf{A}} = \sqrt{\det \mathbf{B}'\mathbf{B}}$ where superscript $'$ denotes the vector or matrix transpose. This quantity is also called the determinant of the lattice and is denoted by $\det \Lambda$. The fundamental parallelepiped for a two-dimensional lattice is shown in Figure 2.3 as the region covered by the dashed line parallelepiped. $\mathcal{P}(B)$ depends on the basis $\mathbf{B}$. It can be observed that if we place a copy of $\mathcal{P}(B)$ at each lattice point in Λ then we obtain tiling of the entire span(Λ) as shown in Figure 2.4.

The (closed) **Voronoi cell**, denoted $\operatorname{Vor}\Lambda$, of an n-dimensional lattice Λ in $\mathbb{R}^m$ is the subset of $\mathbb{R}^m$ containing all points nearer or of equal distance (here with respect to the Euclidean norm) to the lattice point at the origin than to any other lattice point. If the lattice is full rank so that $n = m$ then the volume of the Voronoi cell is equal to the volume of a fundamental parallelepiped, that is, $\det\Lambda$. Otherwise, if the $m > n$ the Voronoi cell is unbounded in those directions orthogonal to the subspace spanned by the basis vectors $\mathbf{b}_1, \ldots, \mathbf{b}_n$. In this case the intersection of the Voronoi cell with this subspace has n-dimensional volume equal to $\det\Lambda$.

The Voronoi cell $\operatorname{Vor}\Lambda$ tessellates $\mathbb{R}^N$ in the sense that

$$\mathbb{R}^N = \bigcup_{\mathbf{x}\in\Lambda} (\operatorname{Vor}\Lambda + \mathbf{t})$$

and $\operatorname{Vor}\Lambda$ and a translate $\operatorname{Vor}\Lambda + \mathbf{t}$ by a lattice point $\mathbf{t} \in \Lambda\backslash\{\mathbf{0}\}$ intersect at most on the boundary of $\operatorname{Vor}\Lambda$. The set $\Lambda\backslash\{\mathbf{0}\}$ denotes those lattice points from Λ not equal to the origin $\mathbf{0}$. In particular, if $\operatorname{int}\Lambda$ denotes the interior of the Voronoi cell, then the intersection of $\operatorname{int}\Lambda$ and $\operatorname{Vor}\Lambda + \mathbf{t}$ is empty for all $\mathbf{t} \in \Lambda\backslash\{\mathbf{0}\}$. This leads to the following simple property that we will find useful.

Remark 1. *If* $\mathbf{t} \in \Lambda$, $\mathbf{u} \in \operatorname{Vor}\Lambda$, $\mathbf{v} \in \operatorname{int}\Lambda$, *and* $\mathbf{u} = \mathbf{v} + \mathbf{t}$, *then* $\mathbf{t} = \mathbf{0}$.

Let r denote the radius of an n-dimensional **Euclidean ball**. The volume V_n of this ball is given as

$$V_n = \frac{\pi^{n/2} r^n}{\Gamma(n/2+1)}$$

where Γ is the Gamma function $\Gamma(n) = (n-1)!$ for $n \in \mathbb{Z}^+$. The radius of this ball can be expressed as

$$r = \frac{(V_n \Gamma(n/2+1))^{1/n}}{\sqrt{\pi}}$$

The probability $P_r(\Lambda, \sigma^2)$ that an independent and identically distributed n-variate Gaussian random variable lies inside the Voronoi cell can be upper bounded by the probability that this n-variate Gaussian random variable lies within a ball of volume

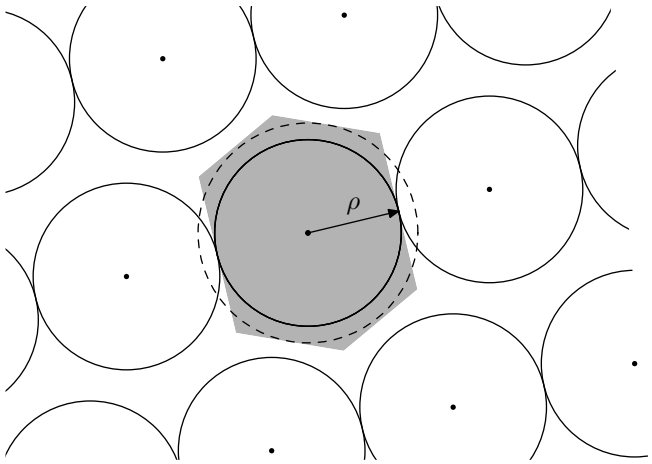

Figure 2.5: The inradius $\rho = d_{\min}/2$ of the 2-dimensional lattice with basis $\mathbf{b}_1 = [3, 0.72]', \mathbf{b}_2 = [0.6, 3.6]'$. The dots are the lattice points. The origin $\mathbf{0}$ is the lattice point in the center of the figure. This lattice has two short vectors. The shaded region shows the Voronoi cell of the lattice. The solid circles exhibit a sphere packing. The dashed circle has area (2-volume) equal to that of the Voronoi cell. The sphere with volume equal to the Voronoi cell is used in the upper bound (5.4).

equal to that of the Voronoi cell [32, Sec. IV.C], i.e.,

$$P_r(\Lambda, \sigma^2) \leq F_n\left(\frac{(\Gamma(n/2+1)\det\Lambda)^{2/n}}{\pi\sigma^2}\right) \tag{2.1}$$

where $F_n(x)$ is the chi-square cumulative distribution function with n degrees of freedom, $\Gamma(x)$ is the gamma function.

The **inradius** or **packing radius** $\rho = d_{\min}/2$ is the length of a point on the boundary of the Voronoi cell that is closest to the origin (Figure 2.5). Equivalently, the inradius is the radius of the largest sphere that fits inside the Voronoi cell. It is also the radius of the largest sphere that can be centered at each lattice point such that no two spheres intersect. Such an arrangement of spheres is called a **sphere packing** (Figure 2.5).

Let Λ be an n-dimensional lattice and let H be the n-dimensional subspace spanned by its lattice points. The **dual lattice** of Λ, denoted Λ^*, contains those points from H that have integer inner product with all points from Λ, that is,

$$\Lambda^* = \{\mathbf{x} \in H \ ; \ \mathbf{x}'\mathbf{y} \in \mathbb{Z} \text{ for all } \mathbf{y} \in \Lambda\}.$$

The determinant of a lattice and its dual are reciprocals, that is, $\det \Lambda = (\det \Lambda^*)^{-1}$ [36, p. 10]. A lattice and its dual have interesting properties when intersected with or projected onto a subspace.

Proposition 1. *Let $\Lambda \subset \mathbb{R}^n$ be an n dimensional lattice, and let H be a $n-k$ dimensional subspace of $\mathbb{R}^n$. Let $H^\perp$ be the k dimensional space orthogonal to H and let p be the orthogonal projection onto H. The set $\Lambda \cap H$ is an $n-k$ dimensional lattice if and only if $\Lambda \cap H^\perp$ is a k dimensional lattice. Moreover, if $\Lambda \cap H$ is an $n-k$ dimensional lattice then:*

1. *The dual of $\Lambda \cap H$ is the orthogonal projection of Λ^* onto H, that is, $(\Lambda \cap H)^* = p(\Lambda^*)$.*
2. *The determinants of Λ, $\Lambda \cap H$ and $\Lambda^* \cap H^\perp$ are related by $\det(\Lambda)\det(\Lambda^* \cap H^\perp) = \det(\Lambda \cap H)$.*

Proof. Proposition 1.3.4 and Corollary 1.3.5 of [37]. □

For the purpose of range estimation we will be particularly interested in Proposition 1 when Λ is the integer lattice $\mathbb{Z}^n$ and $k = 1$. We state this special case in the following corollary.

Corollary 1. *Let $\mathbf{v} \in \mathbb{Z}^n$, let H be the $n-1$ dimensional subspace orthogonal to $\mathbf{v}$, and let*

$$\mathbf{Q} = \mathbf{I} - \frac{\mathbf{v}\mathbf{v}'}{\mathbf{v}'\mathbf{v}} = \mathbf{I} - \frac{\mathbf{v}\mathbf{v}'}{\|\mathbf{v}\|^2}$$

be the $n \times n$ orthogonal projection matrix onto H. The set of vectors $\mathbb{Z}^n \cap H$ is an $n-1$ dimensional lattice with determinant

$$\det(\mathbb{Z}^n \cap H) = \|\mathbf{v}\|$$

and dual lattice

$$(\mathbb{Z}^n \cap H)^* = \{\mathbf{Q}\mathbf{z} \; ; \; \mathbf{z} \in \mathbb{Z}^n\}.$$

Given a vector $\mathbf{y} \in \mathbb{R}^m$, a problem of interest is to find a lattice point $\mathbf{x} \in \Lambda$ such that the squared Euclidean norm

$$\|\mathbf{y} - \mathbf{x}\|^2 = \sum_{i=1}^{m} (y_i - x_i)^2$$

is minimised. This is called the **closest lattice point problem** (or **closest vector problem**) and a solution is called a **closest lattice point** (or simply **closest point**) to $\mathbf{y}$ [35, 38–40]. The closest lattice point problem and the Voronoi cell are related in that $\mathbf{x} \in \Lambda$ is a closest point to $\mathbf{y}$ if and only if $\mathbf{y} - \mathbf{x} \in \operatorname{Vor} \Lambda$.

A **short vector** in a lattice Λ is a lattice point of minimum nonzero Euclidean length, that is, a lattice point of length

$$d_{\min} = \min_{\mathbf{x} \in \Lambda \setminus \{\mathbf{0}\}} \|\mathbf{x}\|^2.$$

The length $d_{\min}$ of a short vector is the smallest distance between any two lattice points.

The closest lattice point problem has numerous engineering applications. For example, the closest lattice point corresponds to the minimum distortion point when a lattice is used as a quantiser and it is called lattice decoding when a lattice is used to construct codes [41, 42]. The problem also occurs in communications systems involving multiple antennas [43] and has also found applications to circular statistics [44], single frequency estimation [45], and related signal processing problems [46–49]. In the context of range estimation from phase observations, the closest lattice point problem has been applied by Teunissen [4], Hassibi and Boyd [32] and more recently Li et. al. [33, 50].

The closest lattice point problem is known to be NP-hard under certain conditions when the lattice itself, or rather a basis thereof, is considered as an additional input parameter [51–53]. Nevertheless, algorithms exist that can compute a closest lattice point in reasonable time if the dimension is small (less that about 60) [35, 39]. Although the problem is NP-hard in general, fast algorithms are known for specific highly regular lattices [38, 40, 54, 55]. For the purpose of range estimation the dimension of the lattice will be $N - 1$ where N is the number of frequencies transmitted. Usually N is not

large. In this case general purpose algorithms for computing a closest lattice point, such as those described in [35], are fast.

2.2 Range Estimation and Phase Ambiguity Problem

Range (or distance) estimation is an important component of modern technologies such as electronic surveying [1, 2] and global positioning systems (GPS) [3, 4]. Common methods of range estimation are based upon received signal strength [7, 8], time of flight (or time of arrival) [9, 10], and phase of arrival [1, 18, 33]. This thesis focuses on the phase of arrival method which provides the most accurate range estimates in many applications. Phase of arrival has become the technique of choice in modern high precision surveying and global positioning [3, 4, 16]. A difficulty with phase of arrival is that only the principal component of the phase can be observed, that is, the observed value of the phase lies within the interval $[-\pi, \pi)$. This limits the range that can be unambiguously estimated. One approach to address this problem is to utilise signals of multiple different wavelengths and observe the phase at each. The range can then be measured within an interval of length equal to the least common multiple of these wavelengths.

Range estimators from such observations have been studied by numerous authors [4, 18, 19, 27, 28, 31–33]. Techniques include the beat wavelength method of Towers et. al. [18, 19], the method of excess fractions [22], and methods based on the Chinese Remainder Theorem (CRT) [24–31, 56–59]. Least squares/maximum likelihood and maximum a posteriori (MAP) estimators of range have been studied by Teunissen [4], Hassibi and Boyd [32], and more recently by Li et. al. [33]. A key realisation is that least squares and MAP estimators can be computed by solving a problem from computational number theory known as the *closest lattice point problem* [35, 60]. Teunissen [4] appears to have been the first to have realised this connection.

This thesis focuses on the least squares estimation of range from multiple phase observations that will be discussed in Chapter 3. In the remaining of this chapter we describe some important range estimation techniques from multiple phase measurements. A good understanding of these methods will be helpful for comparison with the least squares range estimator in the later chapters.

2.3 Range Estimation Techniques

In this section we describe some important range estimators that employ multiple phase observations to estimate the unknown range. These estimators are based upon: (i) the beat wavelength method, (ii) the method of excess fractions, (iii) the CRT based method, and (iv) the least squares range estimator. We first briefly describe the notation and system model used in this work.

Suppose that a transmitter sends a signal of the form

$$x(t) = \sin(2\pi f t + 2\pi\phi) \tag{2.2}$$

of known phase ϕ and frequency f in Hertz. The signal is assumed to propogate by line of sight to a reciever resulting in the signal

$$y(t) = \alpha x(t - r_0/c) + w(t) = \alpha \sin(2\pi f t + 2\pi\theta) + w(t) \tag{2.3}$$

where r_0 is the distance (or range) in meters between receiver and transmitter, c is the speed at which the signal propagates in meters per second, α is the amplitude of the received signal, $w(t)$ represents noise,

$$\theta = \phi - \frac{f}{c} r_0 = \phi - \frac{r_0}{\lambda} \tag{2.4}$$

is the phase of the received signal, and $\lambda = c/f$ is the wavelength. Alternatively, the transmitter and receiver could be in the same location and the receiver obtains the

signal after being reflected off a target. In this case the range of the target would be $r_0/2$.

Our aim is to estimate r_0 from the signal $y(t)$. To do this we first calculate an estimate $\hat{\theta}$ of the principal component of the phase θ. In optical ranging applications $\hat{\theta}$ might be given by an interferometer. In sonar or radio frequency ranging applications $\hat{\theta}$ might be obtained from the complex argument of the demodulated signal $y(t)e^{-2\pi jft}$. Whatever the method of phase estimation, the range r_0 is related to the phase estimate $\hat{\theta}$ by the phase difference

$$Y = \langle \phi - \hat{\theta} \rangle = \langle r_0/\lambda + \Phi \rangle \tag{2.5}$$

where Φ represents phase noise and $\langle x \rangle = x - \left\lfloor x + \frac{1}{2} \right\rfloor$ where $\lfloor x \rfloor$ denotes the greatest integer less than or equal to x. For all integers k,

$$Y = \langle r_0/\lambda + \Phi \rangle = \langle (r_0 + k\lambda)/\lambda + \Phi \rangle \tag{2.6}$$

and so the range is identifiable only if r_0 is assumed to lie in an interval of length λ. A natural choice is the interval $[0, \lambda)$. This poses a problem if the range r_0 is larger than the wavelength λ. To alleviate this, a common approach is to transmit multiple signals $x_n(t) = \sin(2\pi f_n t + 2\pi\phi)$ for $n = 1, \ldots, N$, each with a different frequency f_n. Now N phase estimates $\hat{\theta}_1, \ldots, \hat{\theta}_N$ are computed along with phase differences

$$Y_n = \langle \phi - \hat{\theta}_n \rangle = \langle r_0/\lambda_n + \Phi_n \rangle \qquad n = 1, \ldots, N \tag{2.7}$$

where $\lambda_n = c/f_n$ is the wavelength of the nth signal and $\Phi_1, \ldots, \Phi_N$ represent phase noise. The relationship between the unknown integer multiples or wrapping variables (also called the fringe order in optical metrology) z_n, the phase differences (also called the fractional fringe order in optical metrology) Y_n and the unknown range r_0 is given by

$$r_0 = (z_n + Y_n)\lambda_n \quad n = 1, \ldots, N \tag{2.8}$$

In the following subsections we briefly describe the beat wavelength method, the method of excess fractions and the CRT based method to estimate r_0.

2.3.1 The Beat Wavelength Method

Beat wavelength method introduced by Wyant [**?**] provides direct calculation of the wrapping variables. The maximum measurable distance using the beat wavelength approach is equal to the largest beat wavelength. In the following we describe the two wavelength and multi-wavelength interferometry using the beat wavelength method.

Two Wavelength Interferometry

In two wavelength interferometry two measurement wavelengths λ_0 and λ_1 are used to measure the unknown range. Let ϕ_0 and ϕ_1 be the wrapped phases and z_0 and z_1 be the wrapping variables (or integer fringe orders) at wavelengths λ_0 and λ_1. In beat wavelength method, the beat wavelength and the beat phase are defined respectively as

$$\Lambda_{01} = \frac{\lambda_0 \lambda_1}{(\lambda_1 - \lambda_0)}$$

and

$$\Phi_{01} = \phi_1 - \phi_0,$$

which is normally wrapped into the interval $[-\pi, \pi)$ and the fringe order (wrapping variable) is $Z_{01} = z_0 - z_1$. The maximum measurable distance $r_{\max}$ with conventional beat wavelength method is $r_{\max} \leq \Lambda_{01}$. In this case $Z_{01} = 0$ and the unknown range r_0 is

$$r_0 = \left(z_0 + \frac{\phi_0}{2\pi} \right) \lambda_0 = \left(\frac{\Phi_{01}}{2\pi} \right) \Lambda_{01}.$$

The fringe order (wrapping variable) at λ_0 can be found from

$$z_0 = \left\lceil \frac{\Phi_{01}}{2\pi} \frac{\Lambda_{01}}{\lambda_0} - \frac{\phi_0}{2\pi} \right\rfloor.$$

The noise present in the phase measurement is amplified due to the fact that the beat phase Φ_{01} is scaled by Λ_{01}/λ_0.

Multi-wavelength Interferometry

When multiple beat wavelengths are used for range estimation, the longest one determines the unambiguous measurement range. The measurement uncertainty is dependent upon the ratio of the beat wavelength to the measurement wavelength. Therefore, the shortest beat wavelength gives the lowest uncertainty. In multi-wavelength Interferometry the result from one beat wavelength is typically used to calculate the fringe order (or wrapping variable) of the next smaller beat wavelength. In beat wavelength method the unknown range r_0 is related to the wavelengths as follows

$$r_0 = (Z_{0i} + \Phi_{0i})\Lambda_{0i}$$

where $Z_{0i} = z_0 - z_i$, $\Phi_{0i} = \Phi_0 - \Phi_i$ and Λ_{0i} is called the *beat wavelength* defined as

$$\Lambda_{0i} = \frac{\Lambda_i \Lambda_0}{\Lambda_i - \Lambda_0}$$

A series of steps are carried out to calculate the wrapping variable z_0 at the smallest wavelength λ_0. In the first step, r_0 is estimated using the information available at the largest synthetic wavelength Λ_{01}. As the maximum measurable distance cannot be larger than the largest synthetic wavelength, it follows that the wrapping variable Z_{01} at the largest synthetic wavelength is equal to zero. Therefore, we have

$$r_0 = (Z_{01} + \Phi_{01})\Lambda_{01} = \Phi_{01}\Lambda_{01}$$

The results from first step are then used to calculate the wrapping variable for the next smaller synthetic wavelength Λ_{02}. The results from second step are then used to calculate the wrapping variable for the next smaller synthetic wavelength Λ_{03} and so on in the same manner using

$$(Z_{0(i+1)} + \Phi_{0(i+1)})\Lambda_{0(i+1)} = (Z_{0i} + \Phi_{0i})\Lambda_{0i},$$

as

$$Z_{0(i+1)} = \left\lceil (Z_{0i} + \Phi_{0i}) \frac{1-\alpha_{i+1}}{1-\alpha_i} - \Phi_{0(i+1)} \right\rfloor$$

with

$$(1-\alpha_i) = \frac{\lambda_{0(N-1)}}{\Lambda_{0i}}$$

where α_i is a dimensionless quantity, $0 < \alpha_i < 1$. α_i is introduced in [Give reference] to show the effect of the centre wavelengths. In the final step, the wrapping variable at the smallest measurement wavelength is carried out using

$$z_0 = \left\lceil (Z_{0(N-1)} + \Phi_{0(N-1)}) sf - \Phi_0 \right\rfloor$$

where sf is so called scaling factor given as

$$sf = \frac{\Lambda_{0(N-1)}}{\lambda_0} = \frac{\lambda_{N-1}}{\lambda_{N-1} - \lambda_0}$$

The coefficients α_i and sf are introduced to simplify and generalise the problem without referring to the wavelengths. Several sets of wavelengths may generate the same values of α_i and sf. In the presence of noise, the actual values of the coefficients α_i and sf determine the measurement reliability of the multi-wavelength interferometer. The coefficients α_i and sf can be adjusted to choose an optimised set of wavelengths for an optimised performance of the interferometer. Hierarchical approaches [Insert References] are one class of optimum wavelength selection for multiple beat wavelength interferometry.

The length of the beat wavelength is inversely proportional to the wavelength separation, and hence to measure a longer distance the two measurement wavelengths must be very close to each other. For example, a wavelength separation of approximately 2 pico meters generates a beat wavelength of 1 meter in C band. This small separation represents a limitation for practical systems and hence the beat wavelength method is not applicable to long range metrology. Hence, extended beat wavelength methods [Insert References] have developed to increase the unambiguous measurement range.

2.3.2 The Method of Excess Fractions

Another popular method to estimate the wrapping variables is the Michelson-Benoit's method of Excess Fractions (EF). It consists of a comparison of the measured phases at each wavelength to estimate the unknown distance r_0. The relation between the unknown wrapping variables z_n, the phase differences Y_n and the unknown range r_0 is given by (2.8). The wrapping variable at the smallest wavelength z_0 must lie within the interval $[0, m_{0\max}]$, with $m_{0\max} = \lceil \mathrm{UMR}/\lambda_0 - 1 \rfloor$. It is possible to represent (2.8) as

$$r_0 = (Z_{0i} + \Phi_{0i})\Lambda_{0i},$$

where $Z_{0i} = z_0 - z_i$, $\Phi_{0i} = \Phi_0 - \Phi_i$ and Λ_{0i} is called the *beat wavelength* defined as

$$\Lambda_{0i} = \frac{\Lambda_i \Lambda_0}{\Lambda_i - \Lambda_0}$$

In EF, a residual error corresponding to the smallest measurement wavelength λ_0 is defined in order to find the correct wrapping variable z_0. To do this, the wrapping variable at the ith wavelength z_i is first calculated using

$$z_i = (z_0 + \phi_0)\frac{\lambda_0}{\lambda_i} - \phi_i.$$

The residual error r_i is then defined as the difference between this calculated value of z_i and the nearest integer of this value, i.e.,

$$r_i(z_0) = \left\langle (z_0 + \phi_0)\frac{\lambda_0}{\lambda_i} - \phi_i \right\rangle \tag{2.9}$$

We can also express the residual error in terms of the beat wavelength as

$$(z_0 + \phi_0)\lambda_0 = (Z_{0i} + \Phi_{0i})\Lambda_{0i},$$

hence,

$$r_i(z_0) = \left\langle -\frac{(z_0 + \phi_0)\lambda_0}{\Lambda_{0i}} + Z_{0i} \right\rangle \tag{2.10}$$

Equations (2.9) and (2.10) are equivalent. For convenience a dimensionless scaling factor $sf_i = \Lambda_{0i}/\lambda_0$ is introduced, where $sf_i > 1$. Hence

$$r_i(z_0) = \left\langle -\frac{(z_0 + \phi_0)}{sf_i} + Z_{0i} \right\rangle \tag{2.11}$$

In general case, when N measurement wavelengths are used, an overall residual error $R(z_0)$ can be defined as

$$R(z_0) = \sqrt{\sum_{i=1}^{N-1} |r_i(m_0)|^2}. \tag{2.12}$$

Eq. (2.12) must be evaluated for all possible values of z_0. Then the most likely solution for the wrapping variable at the smallest measurement wavelength z_0 and hence the range r_0 is identified by the z_0 that results in minimum overall residual error in (2.12).

2.3.3 The CRT Based Method

The CRT based method for range estimation is based upon the Chinese remainder theorem (CRT). The Chinese remainder theorem can uniquely solve any pair of congruences that have relatively prime moduli.

Let r_0 be the unknown range that we want to estimate and let $\lambda_1, \lambda_2, \ldots, \lambda_N$ be pairwise relatively prime wavelengths, and $r_1, r_2, \ldots, r_N$ be remainders of r_0 modulo λ_n, for $n = 1, 2, \ldots, N$. Then the system of congruences

$$r_0 = r_n \pmod{\lambda_n} \quad 1 \leq n \leq N$$

has a unique solution modulo $P = \lambda_1 \times \lambda_2 \times \ldots \times \lambda_N$, which is given by

$$r_0 = r_1 v_1 y_1 + r_2 v_2 y_2 + \ldots + r_n v_n y_n \pmod{P},$$

where $v_n = P/\lambda_n$ and $y_n = v_n^{-1} \pmod{\lambda_n}$ for $1 \leq n \leq N$.

This is called the classical CRT. If any pair of moduli λ_i have gcd G, then the CRT has the form, described in [24], called the traditional CRT or general CRT. However, it

is well known that CRT is not robust, i.e., a small error in remainders results in a large error in the estimated range. One of the methods to resist these remainder errors is to assume that all the wavelengths λ_n have a common gcd $G > 1$, then the estimation of range is robust to remainder errors. In the following we briefly describe this kind of CRT based range estimator that leads to the searching based robust CRT based range estimators in [27, 58] and then to a closed form robust CRT in [29].

Let

$$\Gamma_n = \lambda_n/G, \quad n = 1, 2, \ldots, N.$$

Then Γ_n, for $n = 1, 2, \ldots, N$, are co-prime, i.e. the gcd of any pair Γ_m and Γ_n for $m \neq n$ is 1. Define $\Gamma = \Gamma_1\Gamma_2 \cdots \Gamma_N$ and let

$$\gamma_n = \Gamma_1 \cdots \Gamma_{n-1}\Gamma_{n+1} \cdots \Gamma_N = \Gamma/\Gamma_n.$$

Obviously, Γ_n and γ_n are co-prime. So the modular multiplicative inverse of γ_n and Γ_n exists. Denote it by $\bar{\gamma}_n$, i.e.,

$$\bar{\gamma}_n\gamma_n \equiv 1 \mod \Gamma_n \quad \text{or} \quad \bar{\gamma}_n\gamma_n + k\Gamma_n = 1,$$

where $k \in \mathbb{Z}$. Let

$$q_n \triangleq \left\lfloor \frac{r_n}{G} \right\rfloor,$$

then

$$r_n = q_nG + c$$

where $c = r_0 \bmod G$ is the common remainder of r_n modulo G for $1 < n < N$. Define

$$R_0 \triangleq \lfloor r_0/G \rfloor.$$

Then using results from the classical CRT, we have following conclusion. If $0 \leq R_0 \leq \Gamma$, R can be constructed as

$$R_0 = \sum_{n=1}^{N} \bar{\gamma}_n\gamma_nq_n \bmod \Gamma.$$

Therefore, r_0 can be uniquely reconstructed by

$$r_0 = R_0 G + c.$$

However, it is well known that the CRT is not robust, i.e., a small error from any remainder may result in a large error in the final estimate of r_0. A searching based robust CRT is proposed in [8] [9](These REFERENCES are from the paper A closed form robust CRT and its performance analysis– Nov 2010) to estimate r_0 from erroneous remainders. Let the nth erroneous remainder be

$$\hat{r}_n \triangleq r_n + \Delta r_n$$

where Δr_n denotes the error or noise and it is assumed that $|\Delta r_n| \leq \tau$, where τ is the maximum error level or remainder error bound. According to [27] the reconstruction of r_0 is robust if the remainder error bound τ is less than a quarter of the gcd G of the measurement wavelengths i.e. $\tau < G/4$. Algorithm provided in [58] reduces the computational complexity of the algorithm provided in [27]. Motivated from the results in [27, 58], a closed form robust CRT algorithm and a necessary and sufficient condition on the remainder errors is also provided in [29]. However, these robust CRT algorithms are only valid for the special case when the gcd of all the moduli (wavelengths) is more than one and the remaining integers after division by these wavelengths are co-prime. Recently, a single-stage and a multi-stage CRT [31] is proposed that removes the constraint used in [27, 29, 58], i.e., this CRT algorithm is valid for a general set of wavelengths and is more appealing for practical applications.

2.4 Wavelength Selection Methods

Chapter 3

Basis Construction for Range Estimation by Phase Unwrapping

3.1 Introduction

In this chapter, we consider the problem of estimating the distance, or range, between two locations by measuring the phase of a sinusoidal signal transmitted between the locations. This method is only capable of unambiguously measuring range within an interval of length equal to the wavelength of the signal. To address this problem signals of multiple different wavelengths can be transmitted. The range can then be measured within an interval of length equal to the least common multiple of these wavelengths.

Estimation of the range requires solution of a problem from computational number theory called the *closest lattice point* problem. Algorithms to solve this problem require a *basis* for this lattice. Constructing a basis is non-trivial and an explicit construction has only been given in the case that the wavelengths can be scaled to pairwise relatively prime integers. In this chapter we present an explicit construction of a basis without this assumption on the wavelengths. This is important because the accuracy of the range estimator depends upon the wavelengths. Numerical results indicate that significant improvement in accuracy can be achieved by using wavelengths that cannot be scaled to pairwise relatively prime integers.

The chapter is organised as follows. Section 3.2 presents the system model and derives the least squares range estimator. Section 3.3 shows how the least squares range estimator is given by computing a closest point in a lattice. In Section 3.4 we describe an explicit basis construction method for these lattices. Simulation results are discussed in Section 3.5 and the paper is concluded by suggesting some directions for future research.

3.2 System Model

Consider the problem of estimating the distance between a transmitter and a receiver using phase only measurements. An important component of the system model of the least squares range estimator is the phase noise. The phase noise is often assumed to be Gaussian without proper justification. However, an additive Gaussian assumption about the phase noise is questionable because the principal component of the phase is contained on the interval $[-\pi, \pi)$ (or $[-1/2, 1/2]$ in our notation), but the support of the normal distribution is the entire real line. This section shows that the wrapped normal distribution [61, p. 50] [62, p. 76] [17, p. 47] with support on $[-1/2, 1/2]$ is a reasonable model for the phase noise. For the least squares estimator it happens that the wrapping can be ignored and that the wrapped normal model for the phase noise is actually equivalent to the normal distribution without wrapping. Some authors have stated that the normal assumption is a reasonable approximation when the variance of the phase noise is small [33, 63, 64]. We show the equivalence between the wrapped normal and normal distribution for the least squares range estimator actually holds regardless of the value of the noise variance. In the following we describe system model for range estimation problem followed by the justification of an additive Gaussian noise assumption for the phase noise.

Suppose that a transmitter sends a signal of the form

$$x(t) = \sin(2\pi f t + 2\pi\phi) \tag{3.1}$$

of known phase ϕ and frequency f in Hertz. The signal is assumed to propagate by line of sight to a receiver resulting in the signal

$$y(t) = \alpha x(t - r_0/c) + w(t) = \alpha \sin(2\pi f t + 2\pi\theta) + w(t) \tag{3.2}$$

where r_0 is the distance (or range) in meters between receiver and transmitter, c is the speed at which the signal propagates in meters per second, α is the amplitude of the received signal, $w(t)$ represents noise,

$$\theta = \phi - \frac{f}{c} r_0 = \phi - \frac{r_0}{\lambda} \tag{3.3}$$

is the phase of the received signal, and $\lambda = c/f$ is the wavelength. Alternatively, the transmitter and receiver could be in the same location and the receiver obtains the signal after being reflected off a target. In this case the range of the target would be $r_0/2$.

The receiver is assumed to be *synchronised* by which it is meant that the phase ϕ and frequency f are known to the receiver. Our aim is to estimate r_0 from the signal $y(t)$. To do this we first calculate an estimate $\hat{\theta}$ of the principal component of the phase θ. In optical ranging applications the phase estimate might be given by an interferometer. In sonar or radio frequency ranging applications the signal $y(t)$ might first be sampled. In this case the receiver acquires, say L, samples of the form

$$y(\ell T) = \alpha \sin(2\pi f \ell T + 2\pi\theta) + w(\ell T) \quad \ell = 0, \ldots, L-1 \tag{3.4}$$

where $T < \frac{1}{2f}$ is the sample period in seconds. It could be that the signal is sampled after first being demodulated by an analogue circuit to a lower frequency. In this case $x(t)$ would represent the *baseband* transmitted signal prior to modulation. If a complex heterodyne modulator is used then the real valued signal $x(t)$ from (3.1) might instead be considered as the complex valued signal $x(t) = e^{2\pi j f t}$. This would not fundamentally alter our results. We keep to the real valued setting here because it also covers the case where no modulation is used and the baseband signal is sampled directly. This is likely the case in sonar and low frequency radio ranging applications.

Given samples, a pragmatic phase estimator involves first computing the complex number

$$a = \frac{2j}{L}\sum_{\ell=0}^{L-1} y(\ell T)e^{-2\pi j f \ell T} = \alpha e^{2\pi j\theta} + \alpha e^{-2\pi j\theta} A + W \tag{3.5}$$

where $W = \frac{2j}{L}\sum_{\ell=0}^{L-1} w(\ell T)e^{-2\pi j f \ell T}$ and

$$A = e^{-2\pi j f T(L-1)}\frac{\sin(2\pi f L T)}{L\sin(2\pi f T)}.$$

Observe that $A \to 0$ as the number of samples $L \to \infty$. Put

$$b = a - a^* A = \alpha e^{2\pi j\theta} + X$$

where $X = W - W^* A$ and superscript * denotes the complex conjugate. The phase estimate is

$$\hat{\theta} = \frac{1}{2\pi}\angle b = \langle \theta - \Phi \rangle \tag{3.6}$$

where $\angle$ denotes the complex argument and

$$\Phi = -\frac{1}{2\pi}\angle\left(1 + \frac{e^{-2\pi j\theta}}{\alpha}X\right)$$

is the *phase noise* induced by X [63, 65]. The notation $\langle\cdot\rangle$ denotes the (centered) fractional part of its argument, that is, if $\lceil x \rfloor$ denotes the nearest integer to x with half integer rounded up, then $\langle x\rangle = x - \lceil x \rfloor$. With this definition $\langle x\rangle$ is always in the interval $[-0.5, 0.5)$.

Under the common assumption that the noise samples $w(0), w(T), \ldots, w((L-1)T)$ are independent and identically distributed with zero mean and variance σ^2 it follows that X is a zero mean complex valued random variable with finite variance. Furthermore, as $L \to \infty$, the distribution of $\sqrt{L}X$ can be shown to converge to the circularly symmetric complex normal distribution with independent real and imaginary parts having variance $\sigma^2/2$. This realisation motivates use of the *projected normal distribution* to model the phase noise [61, p. 46][62, p. 81]. However, for the purpose of analysis, it will be more convenient to model the phase noise using the *wrapped normal*

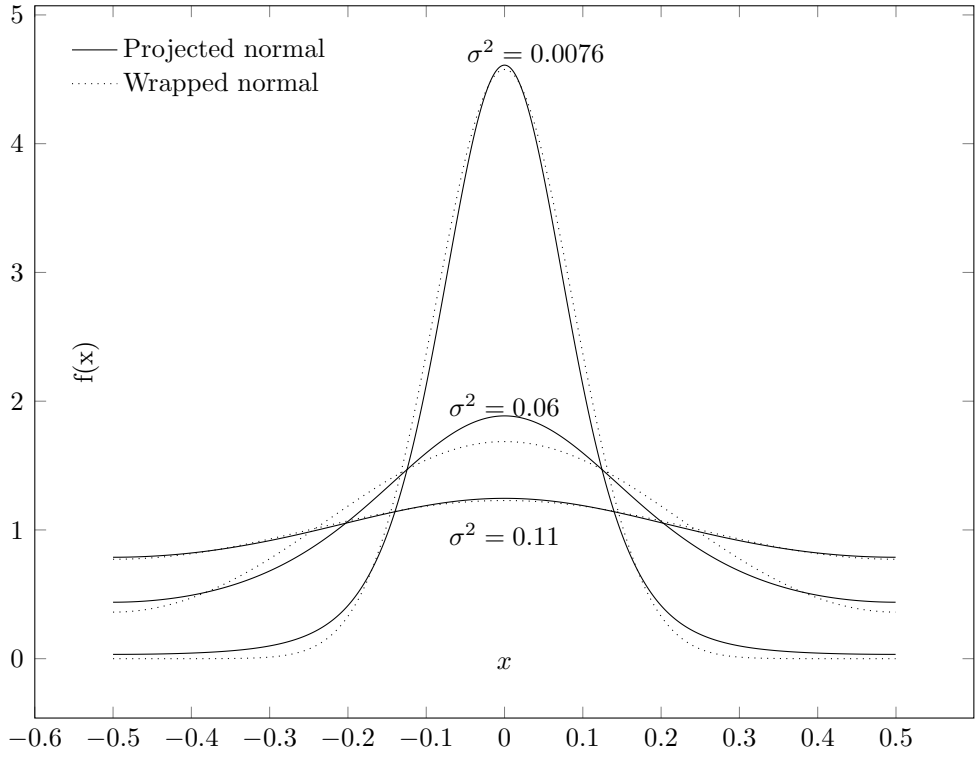

Figure 3.1: Comparison of projected normal and wrapped normal distributions for different values of σ^2.

distribution [61, p. 50][62, p. 76][17, p. 47]. That is, we model the phase noise as $\Phi = \langle \epsilon \rangle$ where ϵ is normally distributed with zero mean. This assumption is reasonable because the projected normal and wrapped normal distributions are similar as observed in Figure 3.1. With this assumption

$$\hat{\theta} = \langle \theta - \Phi \rangle = \langle \theta - \langle \epsilon \rangle \rangle = \langle \theta - \epsilon \rangle \tag{3.7}$$

and so, the phase noise may equivalently be modelled as normally distributed *without wrapping*. This is a highly convenient consequence of the wrapped normal assumption. The assumption of normally distributed phase noise is common in the range estimation literature but is usually made without justification [33, 66]. The assumption is justified by the discussion above.

Our aim is to estimate r_0 from the signal $y(t)$. To do this we first calculate an estimate $\hat{\theta}$ of the principal component of the phase θ. In optical ranging applications $\hat{\theta}$ might be given by an interferometer. In sonar or radio frequency ranging applications

$\hat{\theta}$ might be obtained from the complex argument of the demodulated signal $y(t)e^{-2\pi jft}$. Whatever the method of phase estimation, the range r_0 is related to the phase estimate $\hat{\theta}$ by the phase difference

$$Y = \langle \phi - \hat{\theta} \rangle = \langle r_0/\lambda + \Phi \rangle \tag{3.8}$$

where Φ represents phase noise.For all integers k,

$$Y = \langle r_0/\lambda + \Phi \rangle = \langle (r_0 + k\lambda)/\lambda + \Phi \rangle \tag{3.9}$$

and so ranges r_0 and $r_0 + k\lambda$ result in the same phase difference. For this reason the range is identifiable from the phase only if we assume r_0 to lie in some interval of length λ. A natural choice is the interval $[0, \lambda)$. This poses a problem if the range r_0 is larger than the wavelength λ. To alleviate this, a common approach is to transmit multiple signals $x_n(t) = \sin(2\pi f_n t + 2\pi\phi_n)$ for $n = 1, \ldots, N$, each with a different frequency f_n. Now N phase estimates $\hat{\theta}_1, \ldots, \hat{\theta}_N$ are computed along with phase differences

$$Y_n = \langle \phi - \hat{\theta}_n \rangle = \langle r_0/\lambda_n + \Phi_n \rangle \qquad n = 1, \ldots, N \tag{3.10}$$

where $\lambda_n = c/f_n$ is the wavelength of the nth signal and $\Phi_1, \ldots, \Phi_N$ represent phase noise. Given $Y_1, \ldots, Y_N$, a pragmatic estimator of the range r_0 is a minimiser of the least squares objective function

$$LS(r) = \sum_{n=1}^{N} \langle Y_n - r/\lambda_n \rangle^2 . \tag{3.11}$$

This least squares estimator is also the maximum likelihood estimator under the assumption that the phase noise variables $\Phi_1, \ldots, \Phi_N$ are independent and identically wrapped normally distributed with zero mean [61, p. 50][62, p. 76][17, p. 47].

The objective function LS is periodic with period equal to the smallest positive real number P such that $P/\lambda_n \in \mathbb{Z}$ for all $n = 1, \ldots, N$, that is, $P = \mathrm{lcm}(\lambda_1, \ldots, \lambda_N)$ is the least common multiple of the wavelengths. The least common multiple is the smallest positive integer such that $P/\lambda_1, \ldots, P/\lambda_N$ are all integers. Observe that the ranges r_0 and $r_0 + kP$ for any integer k result in the same phase differences $Y_1, \ldots, Y_N$

and so r_0 can be uniquely identified only within an interval of length P. The range is identifiable if we assume r_0 to lie in an interval of length P. A natural choice is the interval $[0, P)$ and we correspondingly define the least squares estimator of the range r_0 as

$$\hat{r} = \arg \min_{r \in [0,P)} LS(r). \tag{3.12}$$

If λ_n/λ_m is irrational for some n and m then the least common multiple P does not exist and the objective function LS is not periodic. In this thesis we assume this is not the case and that a finite period P does exist. This is a common assumption in the literature and in practice.

3.3 Range estimation and the closest lattice point problem

In this section we show how the least squares range estimator $\hat{r}$ from (3.12) can be efficiently computed by computing a closest point in a lattice of dimension $N-1$. The derivation is similar to those in [44, 45, 48]. Our notation will be simplified by the change of variable $r = P\beta$, where P is the least common multiple of the wavelengths. Put $v_n = P/\lambda_n \in \mathbb{Z}$ and define the function

$$F(\beta) = LS(P\beta) = \sum_{n=1}^{N} \langle Y_n - \beta v_n \rangle^2 .$$

Because LS has period P it follows that F has period 1. If $\hat{\beta}$ minimises F then $P\hat{\beta}$ minimises LS and, because $\hat{r} \in [0, P)$, we have

$$\hat{r} = P(\hat{\beta} - \lfloor \hat{\beta} \rfloor).$$

It is thus sufficient to find a minimiser $\hat{\beta} \in \mathbb{R}$ of F. Observe that

$$\langle Y_n - \beta v_n \rangle^2 = \min_{z \in \mathbb{Z}} (Y_n - \beta v_n - z)^2$$

and so F may equivalently be written

$$F(\beta) = \min_{z_1,\ldots,z_N \in \mathbb{Z}} \sum_{n=1}^{N} (Y_n - \beta v_n - z_n)^2.$$

The integers $z_1, \ldots, z_N$ are often called *wrapping variables* and are related to the number of whole wavelengths that occur over the range r_0 between transmitter and receiver. The minimiser $\hat{\beta}$ can be found by jointly minimising the function

$$F_1(\beta, z_1, \ldots, z_N) = \sum_{n=1}^{N} (Y_n - \beta v_n - z_n)^2$$

over the real number β and integers $z_1, \ldots, z_N$. This minimisation problem can be solved by computing a closest point in a lattice. To see this, define column vectors

$$\begin{aligned}
\mathbf{y} &= (Y_1, \ldots, Y_N)' \in \mathbb{R}^N, \\
\mathbf{z} &= (z_1, \ldots, z_N)' \in \mathbb{Z}^N, \\
\mathbf{v} &= (v_1, \ldots, v_N)' = (P/\lambda_1, \ldots, P/\lambda_N)' \in \mathbb{Z}^N.
\end{aligned}$$

Now

$$F_1(\beta, z_1, \ldots, z_N) = F_1(\beta, \mathbf{z}) = \|\mathbf{y} - \beta\mathbf{v} - \mathbf{z}\|^2.$$

The minimiser of F_1 with respect to β as a function of $\mathbf{z}$ is

$$\hat{\beta}(\mathbf{z}) = \frac{(\mathbf{y} - \mathbf{z})'\mathbf{v}}{\mathbf{v}'\mathbf{v}}.$$

Substituting this into F_1 gives

$$\begin{aligned}
F_2(\mathbf{z}) &= \min_{\beta \in \mathbb{R}} F_1(\beta, \mathbf{z}) \\
&= F_1\big(\hat{\beta}(\mathbf{z}), \mathbf{z}\big) \\
&= \|\mathbf{y} - \hat{\beta(\mathbf{z})}\mathbf{v} - \mathbf{z}\|^2 \\
&= \|\mathbf{y} - \frac{(\mathbf{y} - \mathbf{z})'\mathbf{v}}{\mathbf{v}'\mathbf{v}}\mathbf{v} - \mathbf{z}\|^2 \\
&= \|\mathbf{y} - \mathbf{z} - \frac{\mathbf{v}\mathbf{v}'}{\mathbf{v}'\mathbf{v}}(\mathbf{y} - \mathbf{z})\|^2
\end{aligned}$$

$$= \|\mathbf{Qy} - \mathbf{Qz}\|^2$$

where $\mathbf{Q} = \mathbf{I} - \mathbf{vv}'/\|\mathbf{v}\|^2$ is the orthogonal projection matrix onto the $N-1$ dimensional subspace orthogonal to $\mathbf{v}$. Denote this subspace by H. By Corollary 1 the set $\Lambda = \mathbb{Z}^N \cap H$ is an $N-1$ dimensional lattice with dual lattice $\Lambda^* = \{\mathbf{Qz}\ ;\ \mathbf{z} \in \mathbb{Z}^N\}$. We see that the problem of minimising $F_2(\mathbf{z})$ is precisely that of finding a closest point in the lattice Λ^* to $\mathbf{Qy} \in \mathbb{R}^N$. Suppose we find $\hat{\mathbf{x}} \in \Lambda^*$ closest to $\mathbf{Qy}$ and a corresponding $\hat{\mathbf{z}} \in \mathbb{Z}^N$ such that $\hat{\mathbf{x}} = \mathbf{Q}\hat{\mathbf{z}}$. Then $\hat{\mathbf{z}}$ minimises F_2 and $\hat{\beta}(\hat{\mathbf{z}})$ minimises F. The least squares range estimator in the interval $[0, P)$ is then

$$\hat{r} = P\big(\hat{\beta}(\hat{\mathbf{z}}) - \lfloor \hat{\beta}(\hat{\mathbf{z}}) \rfloor\big). \tag{3.13}$$

It remains to provide a method to compute a closest point $\hat{\mathbf{x}} \in \Lambda^*$ and a corresponding $\hat{\mathbf{z}} \in \mathbb{Z}^N$. In order to use known general purpose algorithms we must first provide a basis for the lattice Λ^* [35]. The projection matrix $\mathbf{Q}$ is *not* a basis because it is not full rank. As noted by Li et. al. [33], a modification of the Lenstra-Lenstra-Lovas algorithm due to Pohst [67] can be used to compute a basis given $\mathbf{Q}$. However, it is preferable to have an explicit construction as described in the next section.

3.4 Basis Construction Method

Li et. al. [33] give a construction under the assumption that the wavelengths $\lambda_1, \ldots, \lambda_N$ can be scaled to relatively prime integers, that is, there exists $c \in \mathbb{R}$ such that $\gcd(c\lambda_k, c\lambda_n) = 1$ for all $k \neq n$.[1] We now remove the need for this assumption and construct a basis in the general case. As a secondary benefit, we believe our construction to be simpler than that in [33]. The following proposition is required.

Proposition 2. *Let* $\mathbf{U}$ *be an* $N \times N$ *unimodular matrix with first column given by* $\mathbf{v}$*. A basis for the lattice* Λ^* *is given by the projection of the last* $N-1$ *columns of* $\mathbf{U}$

[1] The assumption that the wavelengths are pairwise relatively prime is made implicitly in equation (75) in [33].

orthogonally onto H. That is, $\mathbf{Qu}_2, \ldots, \mathbf{Qu}_N$ is a basis for Λ^* where $\mathbf{u}_1, \ldots, \mathbf{u}_N$ are the columns of $\mathbf{U}$.

Because $\mathbf{U}$ is unimodular it is a basis matrix for the integer lattice $\mathbb{Z}^N$. So, every lattice point $\mathbf{z} \in \mathbb{Z}^N$ can be uniquely written as $\mathbf{z} = c_1\mathbf{u}_1 + \cdots + c_N\mathbf{u}_N$ where $c_1, \ldots, c_N \in \mathbb{Z}$. The lattice

$$\begin{aligned}\Lambda^* &= \{\mathbf{Qz} \; ; \; \mathbf{z} \in \mathbb{Z}^N\} \\ &= \{\mathbf{Q}(c_1\mathbf{u}_1 + \cdots + c_N\mathbf{u}_N) \; ; \; c_1, \ldots, c_N \in \mathbb{Z}\} \\ &= \{c_2\mathbf{Qu}_2 + \cdots + c_N\mathbf{Qu}_N \; ; \; c_2, \ldots, c_N \in \mathbb{Z}\}\end{aligned}$$

because $\mathbf{Qu}_1 = \mathbf{Qv} = \mathbf{0}$ is the origin. It follows that $\mathbf{Qu}_2, \ldots, \mathbf{Qu}_N$ form a basis for Λ^*.

To find a basis for Λ^* we require a matrix $\mathbf{U}$ as described by the previous proposition. Such a matrix is given by Li et. al. [33, Eq. (76)] under the assumption that the wavelengths can be scaled to pairwise relatively prime integers. We do not require this assumption here. Because $P = \mathrm{lcm}(\lambda_1, \ldots, \lambda_N)$ it follows that the integers $v_1, \ldots, v_N$ are *jointly* relatively prime, that is, $\gcd(v_1, \ldots, v_N) = 1$. Define integers $g_1, \ldots, g_N$ by $g_N = v_N$ and

$$g_k = \gcd(v_k, \ldots, v_N) = \gcd(v_k, g_{k+1}), \quad k = 1, \ldots, N-1$$

and observe that g_{k+1}/g_k and v_k/g_k are relatively prime integers. For $k = 1, \ldots, N-1$, define the N by N matrix $\mathbf{A}_k$ with m, nth element

$$A_{kmn} = \begin{cases} v_k/g_k & m = n = k \\ g_{k+1}/g_k & m = k+1, n = k \\ a_k & m = k, n = k+1 \\ b_k & m = n = k+1 \\ I_{mn} & \text{otherwise} \end{cases}$$

where $I_{mn} = 1$ if $m = n$ and 0 otherwise. The integers a_k and b_k are chosen to satisfy

$$b_k \frac{v_k}{g_k} - a_k \frac{g_{k+1}}{g_k} = 1 \tag{3.14}$$

and can be computed by the extended Euclidean algorithm. The matrix $\mathbf{A}_k$ is equal to the identity matrix everywhere except at the 2 by 2 block of indices $k \leq m \leq k+1$ and $k \leq n \leq k+1$. The matrix $\mathbf{A}_k$ is unimodular for each k because it has integer elements and because the determinant of the 2 by 2 matrix

$$\begin{vmatrix} v_k/g_k & a_k \\ g_{k+1}/g_k & b_k \end{vmatrix} = b_k \frac{v_k}{g_k} - a_k \frac{g_{k+1}}{g_k} = 1$$

as a result of (3.14). A matrix $\mathbf{U}$ satisfying the requirements of Proposition 2 is now given by the product

$$\mathbf{U} = \prod_{k=1}^{N-1} \mathbf{A}_k = \mathbf{A}_{N-1} \times \mathbf{A}_{N-2} \times \cdots \times \mathbf{A}_1.$$

That $\mathbf{U}$ is unimodular follows immediately from the unimodularity of $\mathbf{A}_1, \ldots, \mathbf{A}_{N-1}$. It remains to show that the first column of $\mathbf{U}$ is equal to $\mathbf{v}$. Let $\mathbf{v}_1, \ldots, \mathbf{v}_{N-1}$ be column vectors of length N defined as

$$\begin{aligned} \mathbf{v}_k &= (v_1, \ldots, v_k, g_{k+1}, 0, \ldots, 0)', \qquad k = 1, \ldots, N-2 \\ \mathbf{v}_{N-1} &= (v_1, \ldots, v_{N-1}, g_N)' = \mathbf{v}. \end{aligned}$$

One can readily check that $\mathbf{v}_{k+1} = \mathbf{A}_{k+1}\mathbf{v}_k$ for all $k = 1, \ldots, N-1$. The first column of the matrix $\mathbf{A}_1$ is $\mathbf{v}_1$ and so, by induction, the first column of the product $\prod_{k=1}^{K} \mathbf{A}_k$ is $\mathbf{v}_K$ for all $K = 1, \ldots, N-1$. It follows that the first column of $\mathbf{U}$ is $\mathbf{v}_{N-1} = \mathbf{v}$ as required.

Let $\mathbf{U}_2$ be the N by $N-1$ matrix formed by removing the first column from $\mathbf{U}$, that is, $\mathbf{U}_2 = (\mathbf{u}_2, \ldots, \mathbf{u}_N)$. By Proposition 2 a basis for Λ^* is given by projecting the columns of $\mathbf{U}_2$ orthogonally to $\mathbf{v}$, that is, a basis matrix for Λ^* is the N by $N-1$ matrix $\mathbf{B} = \mathbf{Q}\mathbf{U}_2$. Given $\mathbf{B}$ a general purpose algorithm [35] can be used to compute

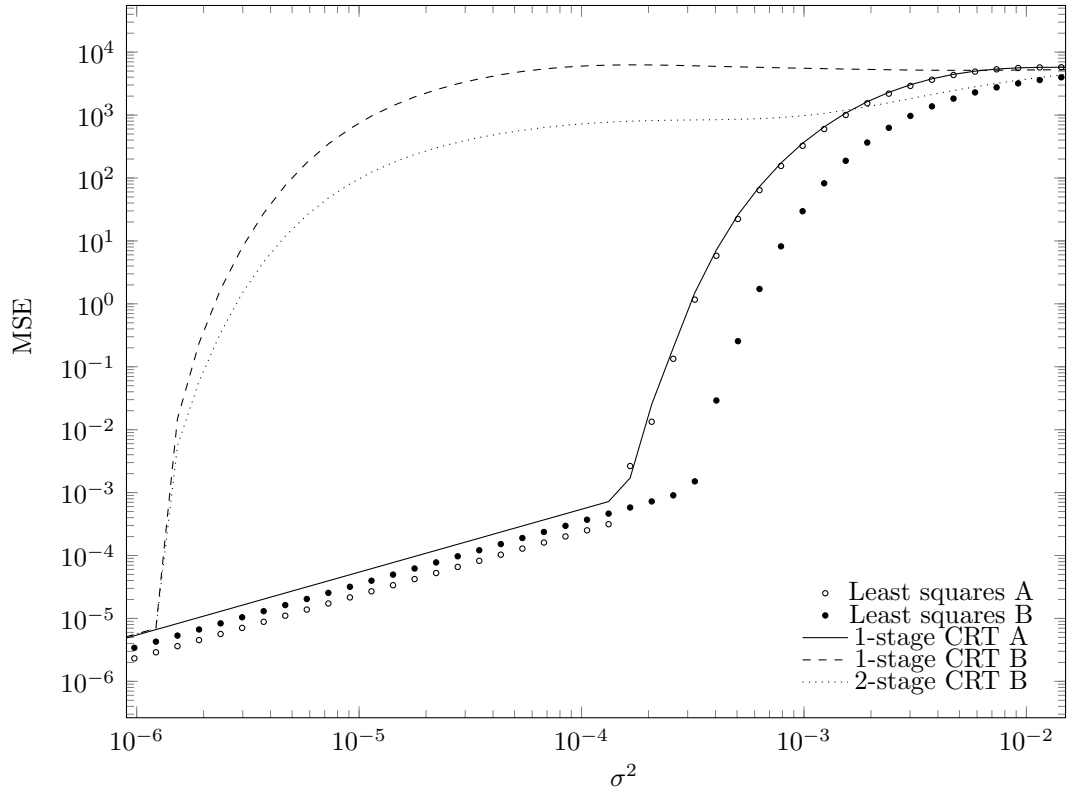

Figure 3.2: Sample mean square error of the least squares and single and multi-stage CRT range estimator with wavelengths A and B.

$\hat{\mathbf{u}} \in \mathbb{Z}^{N-1}$ such that $\hat{\mathbf{x}} = \mathbf{B}\hat{\mathbf{u}}$ is a closest lattice point in Λ^* to $\mathbf{Q}\mathbf{y} \in \mathbb{R}^N$. Now

$$\hat{\mathbf{x}} = \mathbf{B}\hat{\mathbf{u}} = \mathbf{Q}\mathbf{U}_2\hat{\mathbf{u}} = \mathbf{Q}\hat{\mathbf{z}}$$

and so

$$\hat{\mathbf{z}} = \mathbf{U}_2\hat{\mathbf{u}} \in \mathbb{Z}^N. \tag{3.15}$$

The least squares range estimator $\hat{r}$ is then given by (3.13).

3.5 Numerical Results

In this section we present the results of Monte-Carlo simulations with the least squares range estimator and the range estimator based on the single stage and multi-stage CRT algorithms of Xiao et. al. [31]. In each simulation the phase noise variables $\Phi_1, \ldots, \Phi_N$ are wrapped normally distributed, that is, $\Phi_n = \langle \epsilon_n \rangle$ where $\epsilon_1, \ldots, \epsilon_N$ are independent

and normally distributed with zero mean and variance σ^2. In this case, the least squares estimator is also the maximum likelihood estimator. The number of Monte-Carlo trials used for each value of σ^2 is 10^7.

Figure 3.2 shows the sample mean square error for σ^2 in the range 10^{-6} to 10^{-2}. Simulations with $N = 4$ wavelengths are performed and the true range $r_0 = 20\pi$. We consider two different sets of wavelengths

$$A = \{2, 3, 5, 7\}, \quad B = \{\tfrac{210}{79}, \tfrac{210}{61}, \tfrac{210}{41}, \tfrac{210}{31}\}.$$

For both sets the wavelengths are from the interval $[2, 7]$ and $P = 210 = \text{lcm}(A) = \text{lcm}(B)$ so that the identifiable range is the same. The first set A contains pairwise relatively prime integers and so is suitable for the basis of Li et. al. [33], our basis, and the CRT estimator. This set A was used in the simulations in [33]. The second set B is not suitable for the basis of Li et. al. [33] because its elements can not be scaled to pairwise relatively prime integers. To see this, observe that the smallest positive number by which we can multiply the elements of B to obtain integers is $c = \frac{6124949}{210}$. Multiplying the elements by c we obtain the set

$$c \times B = \{77531, 100409, 149389, 197579\}$$

and these elements are not pairwise relatively prime.

Figure 3.2 shows the results of simulations with both sets A and B. The behaviour of the least squares and single-stage CRT estimators is similar for the wavelengths A. No benefit is gained by applying the multi-stage CRT estimator with wavelengths A. When the noise variance σ^2 is small the least squares estimator exhibits slightly smaller mean square error than the CRT estimator. As σ^2 increases the sample mean square error exhibits a 'threshold' effect and increases suddenly. For wavelengths A this threshold occurs at $\sigma^2 \approx 2 \times 10^{-4}$. Different behaviour is exhibited with wavelengths B. When the noise variance σ^2 is small the least squares estimator exhibits slightly smaller mean square error with wavelengths A than with B. However, the threshold with wavelengths B occurs at $\sigma^2 \approx 4 \times 10^{-4}$. Wavelengths B are more accurate than A when

σ^2 is greater than approximately 2×10^{-4}. The single-stage CRT estimator performs comparatively poorly with wavelengths B. The threshold occurs at approximately $\sigma^2 \approx 10^{-6}$. Only small improvement is gained by use of the multi-stage CRT estimator by splitting the wavelength from B into two sets $\{\frac{210}{79}, \frac{210}{31}\}$ and $\{\frac{210}{61}, \frac{210}{41}\}$. Simulations indicate that this is the best splitting of B for the multi-stage CRT estimator.

Figure 3.3 plots the sample mean square error of the least squares range estimator and the range estimator based on the single stage and multi-stage CRT algorithms of Xiao et. al. [31] with $N = 5$ wavelenths. In each simulation the true range $r_0 = 20\pi$. Two different sets of wavelengths are considered,

$$C = \{2, 3, 5, 7, 11\}, \quad D = \{\tfrac{2310}{877}, \tfrac{2310}{523}, \tfrac{2310}{277}, \tfrac{2310}{221}, \tfrac{2310}{211}\}.$$

The wavelengths from both sets are contained in the interval $[2, 11]$ and $P = 2310 = \text{lcm}(C) = \text{lcm}(D)$ so that the identifiable range is the same. The first set C contains pairwise relatively prime integers and so is suitable for the basis of Li et. al. [33], our basis, and the CRT estimator. This set C was used in the simulations in [33]. The second set D is not suitable for the basis of Li et. al. [33] because its elements can not be scaled to pairwise relatively prime integers. To see this, observe that the smallest positive number by which we can multiply the elements of D to obtain integers is $c = \frac{5924555610077}{2310}$. Multiplying the elements by c we obtain the set

$$c \times D = \{6755479601, 11328022199, 21388287401, 26807943937, 28078462607\}$$

and these elements are not pairwise relatively prime.

The behaviour of the least squares and single-stage CRT estimators is similar for the wavelengths C. No benefit is gained by applying the multi-stage CRT estimator with wavelengths C. When the noise variance σ^2 is small the least squares estimator exhibits slightly smaller mean square error than the CRT estimator. As σ^2 increases the sample mean square error exhibits a 'threshold' effect and increases suddenly. For wavelengths C this threshold occurs at $\sigma^2 \approx 6 \times 10^{-5}$.

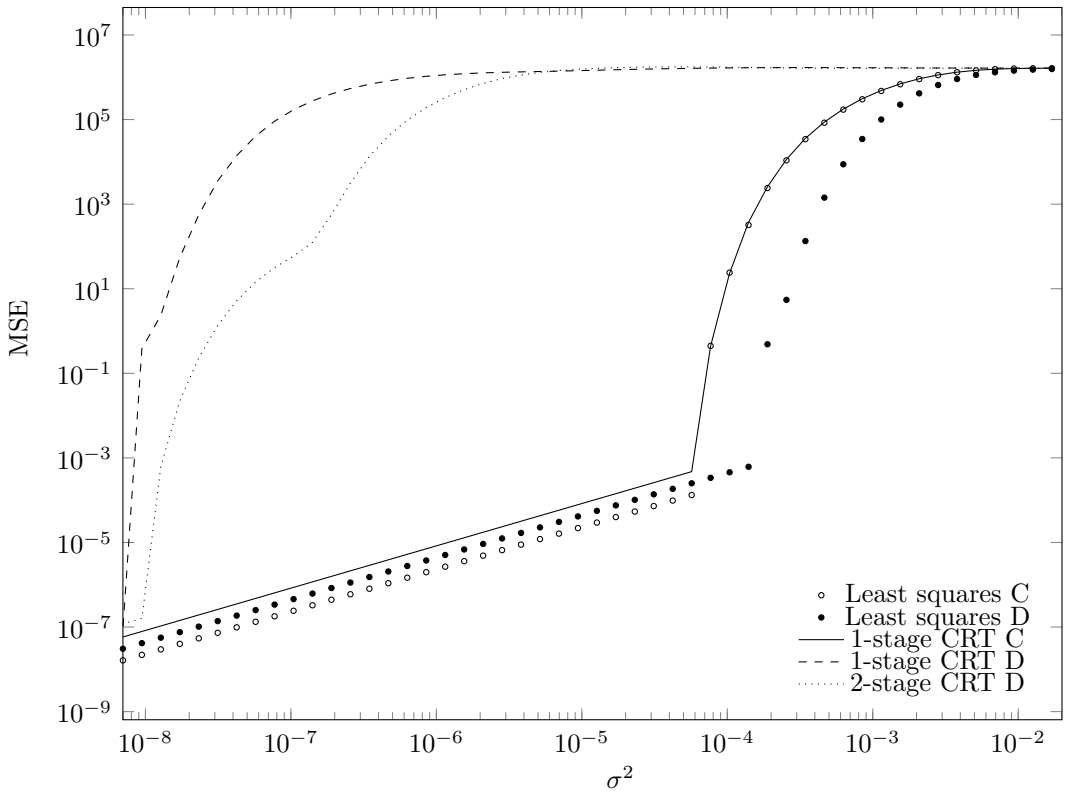

Figure 3.3: Sample mean square error of the least squares range estimator and the range estimator based on the single stage and multi-stage CRT algorithms of Xiao et. al. [31] with $N = 5$ wavelenths.

Different behaviour is exhibited with wavelength D. When the noise variance σ^2 is small the least squares estimator exhibits slightly smaller mean square error with wavelengths C than with D. However, the threshold with wavelengths D occurs at $\sigma^2 \approx 2 \times 10^{-4}$. Wavelengths D are more accurate than C when σ^2 is greater than approximately 6×10^{-5}. The single-stage CRT estimator performs comparatively poorly with wavelengths D. The threshold occurs at approximately $\sigma^2 \approx 7 \times 10^{-9}$. Only small improvement is gained by use of the multi-stage CRT estimator by splitting the wavelengths from D into two sets $\{\frac{2310}{221}, \frac{2310}{211}\}$ and $\{\frac{2310}{877}, \frac{2310}{523}, \frac{2310}{277}\}$. Simulations indicate that this is the best splitting of the wavelengths for the multi-stage CRT estimator in this case.

The wavelengths B and D have been selected based on a heuristic optimisation criterion. The properties of this criterion and the method of selecting these wavelengths are discussed in the following chapters.

3.6 Summary

In this chapter, we considered the problem of estimating the range (or distance) between two locations using the phase of arrival method which provides the most accurate range estimates in many applications. A difficulty with phase of arrival is that only the principal component of the phase can be observed. This limits the range that can be unambiguously estimated to the wavelength of the signal. This problem is addressed by utilising signals of multiple different wavelengths and observing the phase at each.

In this chapter we have considered least squares/maximum likelihood estimation of range from observation of phase at multiple wavelengths. We showed that the least squares range estimator can be computed by solving a problem from computational number theory known as the *closest lattice point problem*. Efficient general purpose algorithms for computing a closest lattice point require a *basis* for the lattice. Constructing a basis for the least squares estimator of range is non-trivial. Bases have previously been constructed under the assumption that the wavelengths can be scaled to relatively prime integers. In this chapter, interesting properties of lattices generated by intersection with or projection onto a subspace are used to construct a basis in the general case. Furthermore, the basis construction method provided in this research is simpler than the existing method provided in [33].

The construction of basis for the general case is important because the accuracy of the range estimator depends upon the wavelengths. Simulations indicate that this can dramatically improve range estimates. These results lead to important problems of characterising the dependence of the least squares range estimator upon the measurement wavelengths and selecting wavelengths to maximise the accuracy of the least squares estimator that is addressed in the following chapters.

Chapter 4

Robustness of the Least Squares Range Estimator

4.1 Introduction

All of the range estimators such as beat wavelength, excess fractions, CRT and least squares either explicitly, or implicitly, make an estimate of so called integer *wrapping variables* related to the whole number of wavelengths that occur over the range. Given estimates of the wrapping variables, an estimate of the range is typically given by linear regression. It is expected that accurate estimators of the wrapping variables will also be accurate estimators of the range. Identification of a criterion that guarantees the correctness of these wrapping variables for the least squares range estimator is important because it provides a basis for selecting wavelengths/frequencies to be used for range estimation. In this chapter we first define the *wrapping variables* and then find a condition on the phase measurement errors that guarantees the correctness of these variables. This finding further motivates the search for methods of selecting wavelengths that can maximise the probability of correctness of these wrapping variables, which is the focus of next chapter.

Robust range estimators from erroneous phase measurements (remainders) for CRT based range estimators are proposed in [29, 58] . They derived an upper bound

τ_{CRT} such that if all the absolute phase measurement errors are less than τ_{CRT}, then the CRT estimator is guaranteed to correctly estimate the wrapping variables. They called τ_{CRT} the *robustness bound*. Their robustness bound holds only if the greatest common divisor (gcd) of all the wavelengths is greater than one and the remaining wavelengths after division by this gcd are co-prime. Recently a robust CRT based range estimator was also proposed in [31] for the general case without the constraint used in [29, 58].

In this chapter we derive a similar upper bound τ_{LS} for the least squares range estimator that indicates the superior performance of the least squares range estimator compared to the CRT estimator. If all absolute phase measurement errors are less than τ_{LS}, then the least squares range estimator is guaranteed to correctly estimate the wrapping variables. The bound is derived from a lattice property called the *inradius*. We find that $\tau_{\text{LS}} > \tau_{\text{CRT}}$ in many cases. This corroborates with existing empirical evidence suggesting that the least squares estimator is often more accurate than those estimators based on the CRT [34].

The chapter is organised as follows. Section 4.2 presents the concept of correct wrapping variables. Section 4.3 derives our upper bound τ_{LS} for the least squares range estimator based upon the inradius of a lattice. Section 4.4 compares the proposed bound τ_{LS} with the bound τ_{CRT} for the CRT based estimator of Xiao et al. [31]. We find that $\tau_{\text{LS}} > \tau_{\text{CRT}}$ in many cases. The results of Monte-Carlo simulations are presented and it is found that the bounds τ_{LS} and τ_{CRT} provide insight about the mean square error of these range estimators.

4.2 Concept of Correct Wrapping Variables

In this section, we further extend the system model presented in 3.2 and define the correct wrapping variables. The understanding of correct wrapping variables is necessary to define the bound τ_{LS} for the least squares range estimator in the next section. Recall that the phase differences can be written in the form

$$Y_n = \langle r_0/\lambda_n + \Phi_n \rangle = r_0/\lambda_n + \Phi_n + \zeta_n$$

where the integers

$$\zeta_n = -\lceil r_0/\lambda_n + \Phi_n \rfloor \qquad n = 1, \ldots, N$$

are called *wrapping variables*. The wrapping variables are related to the number of whole wavelengths that occur over the range r_0 between the transmitter and the receiver. Writing in column vector form

$$\mathbf{y} = r_0\mathbf{w} + \boldsymbol{\Phi} + \boldsymbol{\zeta} \tag{4.1}$$

where the column vectors

$$\mathbf{y} = \begin{pmatrix} Y_1 \\ \vdots \\ Y_N \end{pmatrix} \quad \boldsymbol{\zeta} = \begin{pmatrix} \zeta_1 \\ \vdots \\ \zeta_N \end{pmatrix} \quad \mathbf{w} = \begin{pmatrix} \frac{1}{\lambda_1} \\ \vdots \\ \frac{1}{\lambda_N} \end{pmatrix} \quad \boldsymbol{\Phi} = \begin{pmatrix} \Phi_1 \\ \vdots \\ \Phi_N \end{pmatrix}.$$

The nth element of the vector $\mathbf{w}$ is the reciprocal of the nth wavelength, that is, $w_n = 1/\lambda_n$. Observe P is the smallest positive number such that the vector

$$\mathbf{v} = P\mathbf{w} = (P/\lambda_1, \ldots, P/\lambda_N) \in \mathbb{Z}^N,$$

that is, such that the elements of $\mathbf{v} = P\mathbf{w}$ are all integers. Equivalently, P is the unique positive real number such that the elements of $\mathbf{v}$ are jointly relatively prime, that is, such that

$$\gcd(v_1, \ldots, v_N) = \gcd(P/\lambda_1, \ldots, P/\lambda_N) = 1.$$

Common range estimators, such as the least squares estimator, those estimators based on the CRT, and the method of excess fractions, operate in two stages. In the first stage, an estimate $\hat{\boldsymbol{\zeta}}$ of the wrapping variables $\boldsymbol{\zeta}$ is made. Given $\hat{\boldsymbol{\zeta}}$, an estimate of the range r_0 is typically given by linear regression, that is,

$$\hat{r} = \frac{(\mathbf{y} - \hat{\boldsymbol{\zeta}})'\mathbf{w}}{\mathbf{w}'\mathbf{w}} \tag{4.2}$$

where superscript $'$ indicates the vector or matrix transpose. For any integer k, the ranges r_0 and $r_0 + kP$ are equivalent and so the range estimates $\hat{r}$ and $\hat{r} + kP$ for any integer k are equivalent. It follows that estimates $\hat{\boldsymbol{\zeta}}$ and $\hat{\boldsymbol{\zeta}} + kP\mathbf{w}$ of the wrapping variables are equivalent, because

$$\frac{(\mathbf{y} - \hat{\boldsymbol{\zeta}} + kP\mathbf{w})'\mathbf{w}}{\mathbf{w}'\mathbf{w}} = \hat{r} + kP.$$

For this reason, the estimated wrapping variables $\hat{\boldsymbol{\zeta}}$ are to be considered error free (or correct), if $\hat{\boldsymbol{\zeta}} = \boldsymbol{\zeta} + kP\mathbf{w}$ for some integer k. Because P is the smallest positive integer such that $\mathbf{v} = P\mathbf{w} \in \mathbb{Z}^N$ this occurs if and only if $\mathbf{Q}\hat{\boldsymbol{\zeta}} = \mathbf{Q}\boldsymbol{\zeta}$ where

$$\mathbf{Q} = \mathbf{I} - \frac{\mathbf{w}\mathbf{w}'}{\mathbf{w}'\mathbf{w}} = \mathbf{I} - \frac{\mathbf{v}\mathbf{v}'}{\mathbf{v}'\mathbf{v}} \tag{4.3}$$

is the $N \times N$ orthogonal projection matrix onto the $N - 1$ dimensional subspace orthogonal to $\mathbf{w}$ and $\mathbf{I}$ is the $N \times N$ identity matrix. In what follows, estimates $\hat{\boldsymbol{\zeta}}$ of the wrapping variables $\boldsymbol{\zeta}$ are said to be *correct* if $\mathbf{Q}\hat{\boldsymbol{\zeta}} = \mathbf{Q}\boldsymbol{\zeta}$.

Xiao et al. [31] derived an upper bound

$$\tau_{CRT} = \frac{1}{4c\lambda_{\max}} \min_{1 \le i \le N} \min_{1 \le j \ne i \le N} \gcd(c\lambda_i, c\lambda_j) \tag{4.4}$$

such that if the absolute values of the phase noise are less than τ_{CRT}, then the CRT estimator is guaranteed to correctly estimate the wrapping variables. That is, if $|\Phi_n| < \tau_{\text{CRT}}$ for all $n = 1, \ldots, N$, then $\mathbf{Q}\hat{\boldsymbol{\zeta}} = \mathbf{Q}\boldsymbol{\zeta}$. The value $\lambda_{\max} = \max_n \lambda_n$ is the maximum wavelength and c is a positive real number such the scaled wavelengths $c\lambda_1, \ldots, c\lambda_N$ are all integers. The existance of c is guaranteed by the fact that the wavelengths are assumed to be rationally related, that is, λ_n/λ_k is rational for all n and k.

In the next section we will find a similar upper bound τ_{LS} for the least squares range estimator. It is shown in Section 3.3, that the least squares estimator $\hat{\boldsymbol{\zeta}} \in \mathbb{Z}^N$ of the wrapping variables minimises the quadratic form

$$\|\mathbf{Q}\mathbf{y} - \mathbf{Q}\mathbf{z}\|^2 \qquad \text{over } \mathbf{z} \in \mathbb{Z}^N, \tag{4.5}$$

where $\|\cdot\|$ indicates the Euclidean norm of a vector. Given $\hat{\boldsymbol{\zeta}}$, the least square range estimator $\hat{r}$ is then given by (4.2). It is shown in Section 3.3 how the quadratic form (3.15) can be minimised over $\mathbb{Z}^N$ by computing a closest point in a *lattice*. We will derive the bound τ_{LS} by using a property of this lattice from Section 2.1 called the *inradius*.

4.3 Bound for the least squares range estimator

Recall that the least squares estimate $\hat{\boldsymbol{\zeta}}$ of the wrapping variables $\boldsymbol{\zeta}$ minimises the quadratic form $\|\mathbf{Qy} - \mathbf{Qz}\|^2$ over $\mathbf{z} \in \mathbb{Z}^N$, that is,

$$\|\mathbf{Qy} - \mathbf{Q}\hat{\boldsymbol{\zeta}}\|^2 = \min_{\mathbf{z}\in\mathbb{Z}^N} \|\mathbf{Qy} - \mathbf{Qz}\|^2.$$

It is shown in Chapter 3 that the set

$$\Lambda^* = \{\mathbf{Qz}\ ;\ \mathbf{z} \in \mathbb{Z}^N\}$$

is an $N-1$ dimesional lattice. Thus, $\mathbf{Q}\hat{\boldsymbol{\zeta}}$ is a lattice point in Λ^* and, because

$$\begin{aligned}\|\mathbf{Qy} - \mathbf{Q}\hat{\boldsymbol{\zeta}}\|^2 &= \min_{\mathbf{z}\in\mathbb{Z}^N} \|\mathbf{Qy} - \mathbf{Qz}\|^2 \\ &= \min_{\mathbf{x}\in\Lambda^*} \|\mathbf{Qy} - \mathbf{x}\|^2,\end{aligned}$$

it follows that $\mathbf{Q}\hat{\boldsymbol{\zeta}}$ is a closest lattice point to $\mathbf{Qy}$. Because of this, $\mathbf{Qy} - \mathbf{Q}\hat{\boldsymbol{\zeta}}$ is an element of the Voronoi cell of the lattice Λ^*, that is,

$$\mathbf{Qy} - \mathbf{Q}\hat{\boldsymbol{\zeta}} = \mathbf{Q}(\mathbf{y} - \hat{\boldsymbol{\zeta}}) \in \operatorname{Vor}\Lambda^*.$$

Observe from (4.1) that

$$\begin{aligned}\mathbf{Q}(\mathbf{y} - \hat{\boldsymbol{\zeta}}) &= \mathbf{Q}(r_0\mathbf{w} + \boldsymbol{\Phi} + \boldsymbol{\zeta} - \hat{\boldsymbol{\zeta}}) \\ &= \mathbf{Q}\boldsymbol{\Phi} - \mathbf{Q}(\boldsymbol{\zeta} - \hat{\boldsymbol{\zeta}}).\end{aligned}$$

Suppose that the projection of the phase noise $\mathbf{Q\Phi}$ is in the interior of the Voronoi cell $\operatorname{int}\Lambda$. Then, it follows from Remark 1 of Chapter 2, with $\mathbf{t} = \mathbf{Q}(\boldsymbol{\zeta} - \hat{\boldsymbol{\zeta}})$, $\mathbf{u} = \mathbf{Q}(\mathbf{y} - \hat{\boldsymbol{\zeta}})$, and $\mathbf{v} = \mathbf{Q\Phi}$, that $\mathbf{Q}(\boldsymbol{\zeta} - \hat{\boldsymbol{\zeta}}) = \mathbf{0}$ or equivalently $\mathbf{Q}\boldsymbol{\zeta} = \mathbf{Q}\hat{\boldsymbol{\zeta}}$.

We have found that the least squares estimate $\hat{\boldsymbol{\zeta}}$ of the wrapping variables is correct whenever the projection of the phase noise $\boldsymbol{\Phi}$ orthogonal to $\mathbf{w}$ is contained in the interior of the Voronoi cell, that is, if $\mathbf{Q\Phi} \in \operatorname{int}\Lambda$, then $\mathbf{Q}\hat{\boldsymbol{\zeta}} = \mathbf{Q}\boldsymbol{\zeta}$. Let $\rho = d_{\min}/2$ be the inradius of the lattice Λ^*. If $\|\mathbf{Q\Phi}\| < \rho$ then $\mathbf{Q\Phi} \in \operatorname{int}\Lambda$ and so $\mathbf{Q}\hat{\boldsymbol{\zeta}} = \mathbf{Q}\boldsymbol{\zeta}$. Becasue $\mathbf{Q}$ is an orthogonal projection matrix $\|\boldsymbol{\Phi}\| \geq \|\mathbf{Q\Phi}\|$ and so

$$\begin{aligned} &\|\boldsymbol{\Phi}\| < \rho \\ \implies &\|\mathbf{Q\Phi}\| < \rho \\ \implies &\mathbf{Q}\hat{\boldsymbol{\zeta}} = \mathbf{Q}\boldsymbol{\zeta}, \end{aligned}$$

that is, the least squares estimate $\hat{\boldsymbol{\zeta}}$ of the wrapping variables is correct whenever the Euclidean norm of the phase noise is less than the inradius ρ of the lattice Λ^*. The inradius ρ depends upon the lattice Λ^* which in turn depends upon the wavelengths. This naturally leads to the question of whether it is possible to select wavelengths that maximise the inradius. This is an interesting and nontrivial problem that we intend to investigate in future research.

We now define our bound τ_{LS} for the least squares range estimator. Observe that if

$$|\Phi_n| < \frac{\rho}{\sqrt{N}} = \tau_{LS} \tag{4.6}$$

for all $n = 1, \ldots, N$, then

$$\|\boldsymbol{\Phi}\|^2 = \sum_{n=1}^{N} \Phi_n^2 < \rho^2.$$

It follows that the least squares estimate of the wrapping variables is correct whenever the absolute value of the phase noise $|\Phi_n| < \tau_{\text{LS}} = \rho/\sqrt{N}$ for all $n = 1, \ldots, N$.

We now compare the bound τ_{LS} with the bound τ_{CRT} from (4.4) derived by Xiao et al. [31]. We will find that $\tau_{\text{LS}} > \tau_{\text{CRT}}$ is many cases. We will also find that the bounds τ_{LS} and τ_{CRT} provide insight about the mean square error of these range estimators.

4.4 Numerical Results

This section presents the results of Monte-Carlo simulations with the least squares (LS), CRT, and excess fractions (EF) range estimators. In each simulation, the phase noise $\Phi_1, \ldots, \Phi_N$ are uniformly distributed on the interval $[-\sqrt{3}\sigma, \sqrt{3}\sigma]$ where $\sigma^2 = \mathbb{E}\Phi_n^2$ is the variance. Simulations are performed as σ^2 varies and 10^6 Monte-Carlo trials are used for each value of σ^2. Each trial computes estimated wrapping variables and a corresponding range estimate. From these, we compute an empirical probability that the estimated wrapping variables are correct P_c and the sample mean square error of the range estimator.

Figure 4.1 shows the probability P_c in the case that the $N = 3$ wavelengths are from the set

$$A = \{15 \times 9, 20 \times 9, 18 \times 9\} = \{135, 180, 162\}$$

and the true range $r_0 = 1000$. The maximum measurable range with these wavelengths is $\text{lcm}(A) = 1620$. These wavelengths were also used in [31] for the performance evaluation of the CRT range estimator. For these wavelength the bounds

$$\tau_{\text{LS}} \approx 5.991 \times 10^{-2} \qquad \text{and} \qquad \tau_{\text{CRT}} \approx 3.750 \times 10^{-2}$$

to four significant figures. This suggests that the least squares range estimator has a higher probability of correctly estimating the wrapping variables. This is in agreement with Figure 4.1. As expected, $P_c = 1$ when $\sigma^2 < \tau_{\text{LS}}^2/3 \approx 1.196 \times 10^{-3}$ for the least squares range estimator and when $\sigma^2 < \tau_{\text{CRT}}^2/3 \approx 4.688 \times 10^{-3}$ for the CRT estimator. These bounds on the variance are marked in Figure 4.1 by the vertical solid and dashed lines.

The superior performance of the least squares range estimator is also exhibited by the sample MSE plotted on the bottom of Figure 4.1. The least squares range estimator and the CRT range estimator have similar behaviour when the noise variance σ^2 is small. The MSE exhibits a threshold effect and increases suddenly for sufficiently large σ^2. For the least squares estimator this threshold occurs at approximately 1.74×10^{-3}

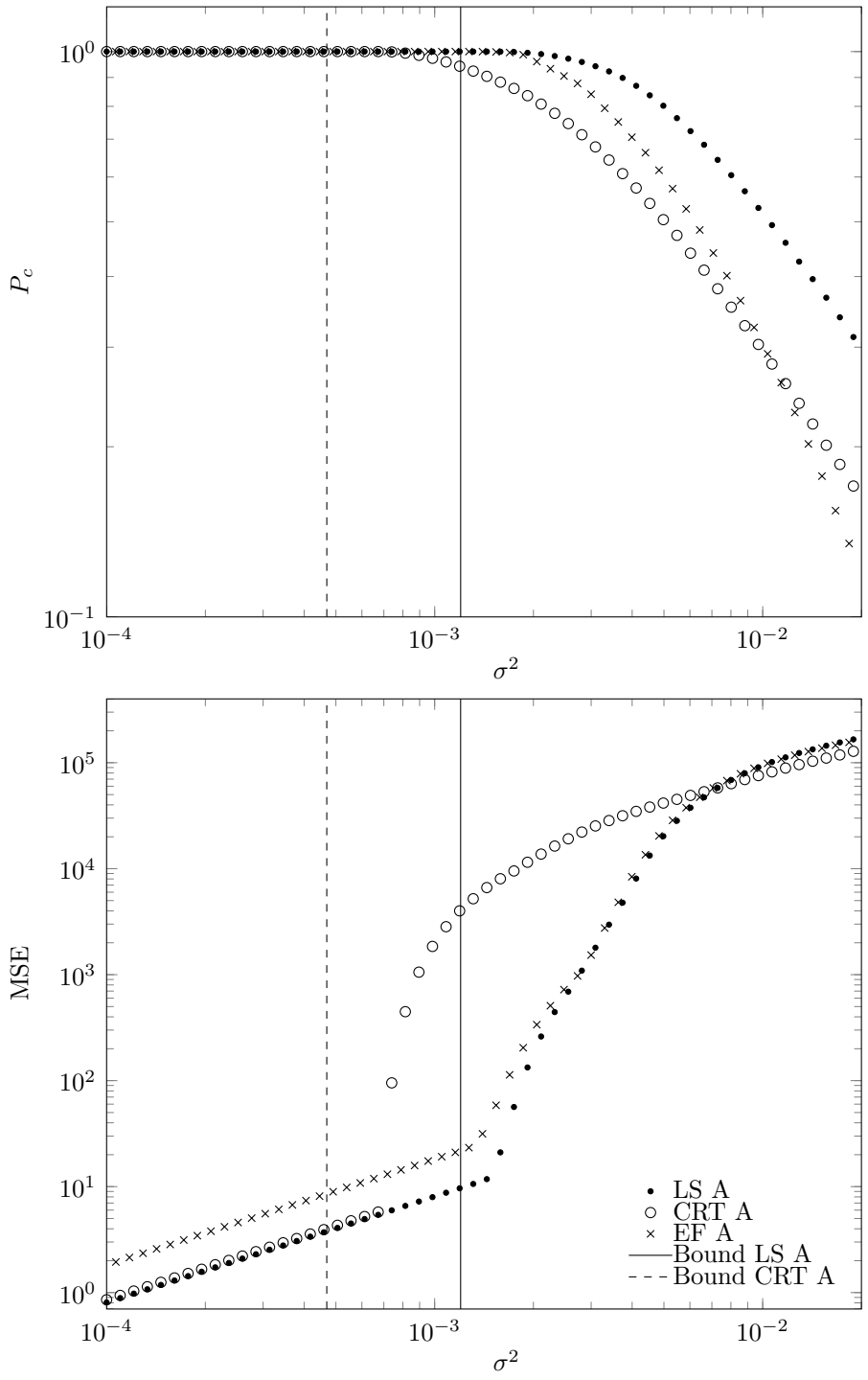

Figure 4.1: Probability of correct estimation of wrapping variables P_c (top), sample mean square error (MSE) (bottom), and bounds on variance with wavelengths A.

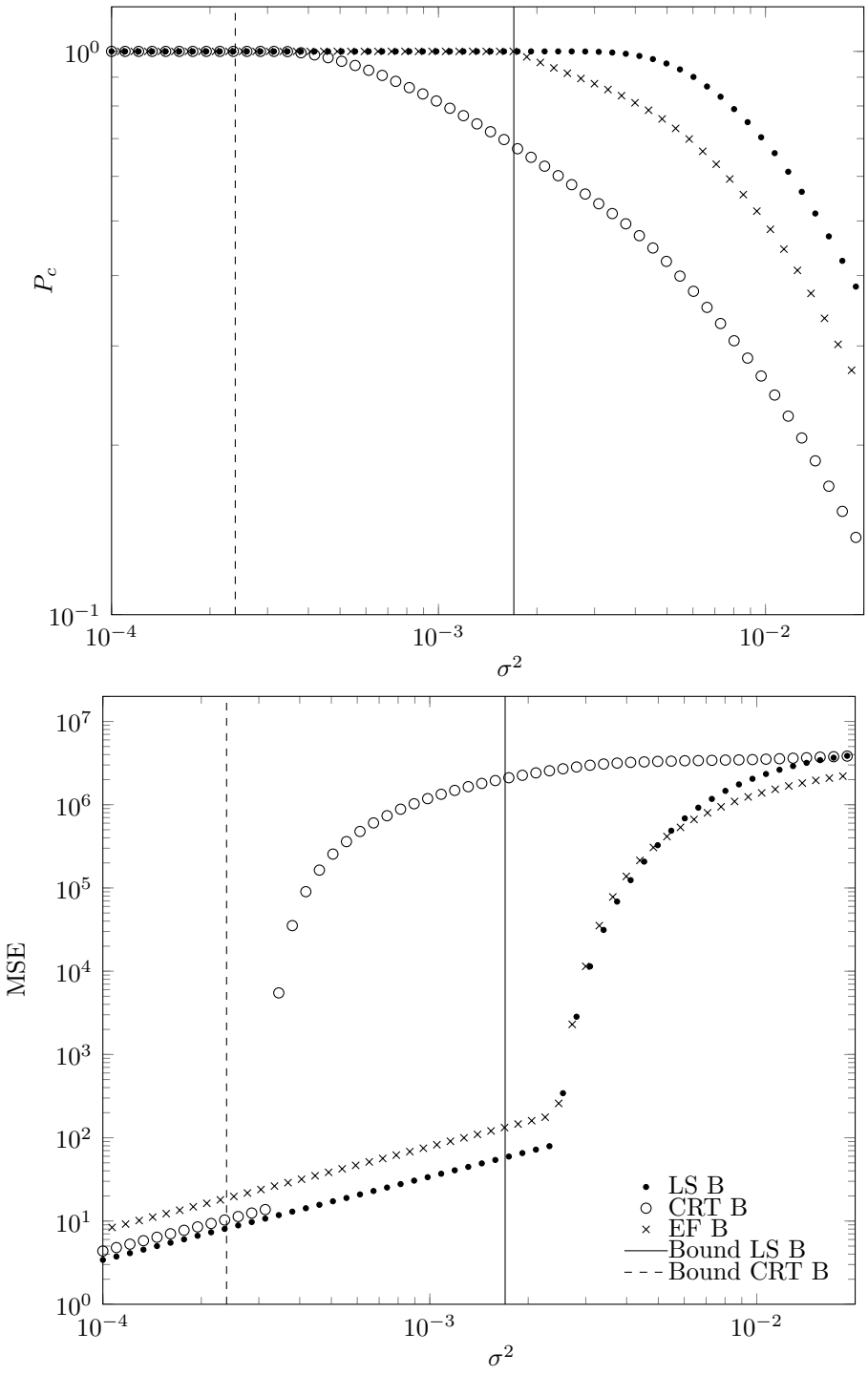

Figure 4.2: Probability of correct estimation of wrapping variables P_c (top), sample mean square error (MSE) (bottom), and bounds on variance with wavelengths B.

whereas for the CRT estimator the threshold occurs at approximately 7.4×10^{-4}. These thresholds are approximated by the bounds on the phase errors $\tau_{\text{LS}}^2/3$ and $\tau_{\text{CRT}}^2/3$. Simulation results are also plotted for the excess fractions (EF) range estimator [22]. No bound equivalent to τ_{LS} or τ_{CRT} is presently known for this estimator.

Figure 4.2 shows the probability P_c when $N = 3$ wavelengths are from the set

$$B = [20 \times 14, 20 \times 18, 20 \times 21, 20 \times 28] = [280, 360, 420, 560].$$

and the true range $r_0 = 2000$. The maximum measurable range with these wavelengths is $\text{lcm}(B) = 5040$. For these wavelength the bounds

$$\tau_{\text{LS}} \approx 7.153 \times 10^{-2} \qquad \text{and} \qquad \tau_{\text{CRT}} \approx 2.678 \times 10^{-2}$$

suggest that the least squares range estimator has a higher probability of correctly estimating the wrapping variables. As expected, $P_c = 1$ when $\sigma^2 < \tau_{\text{LS}}^2/3 \approx 1.705\times10^{-3}$ for the least squares range estimator and when $\sigma^2 < \tau_{\text{CRT}}^2/3 \approx 2.391 \times 10^{-4}$ for the CRT estimator.

The mean square error plot on the bottom of Figure 4.2 also shows the superior performance of the least squares range estimator. The threshold for the least squares estimator in this example occurs at 2.55×10^{-3} whereas for the CRT estimator it occurs at approximately 3.452×10^{-4}. These thresholds are approximated by the bounds on the phase errors as shown in the figure. Figure 4.2 also shows the results for the excess fractions (EF) range estimator.

We have performed a computational search with $N = 2, 3, \text{and } 4$ wavelengths and found that in most cases $\tau_{\text{LS}} > \tau_{\text{CRT}}$. We rarely found examples when $\tau_{\text{LS}} < \tau_{\text{CRT}}$. Such an example is presented in Figure 4.3 for $N = 4$ wavelengths from the set

$$C = [13, 17, 19, 20].$$

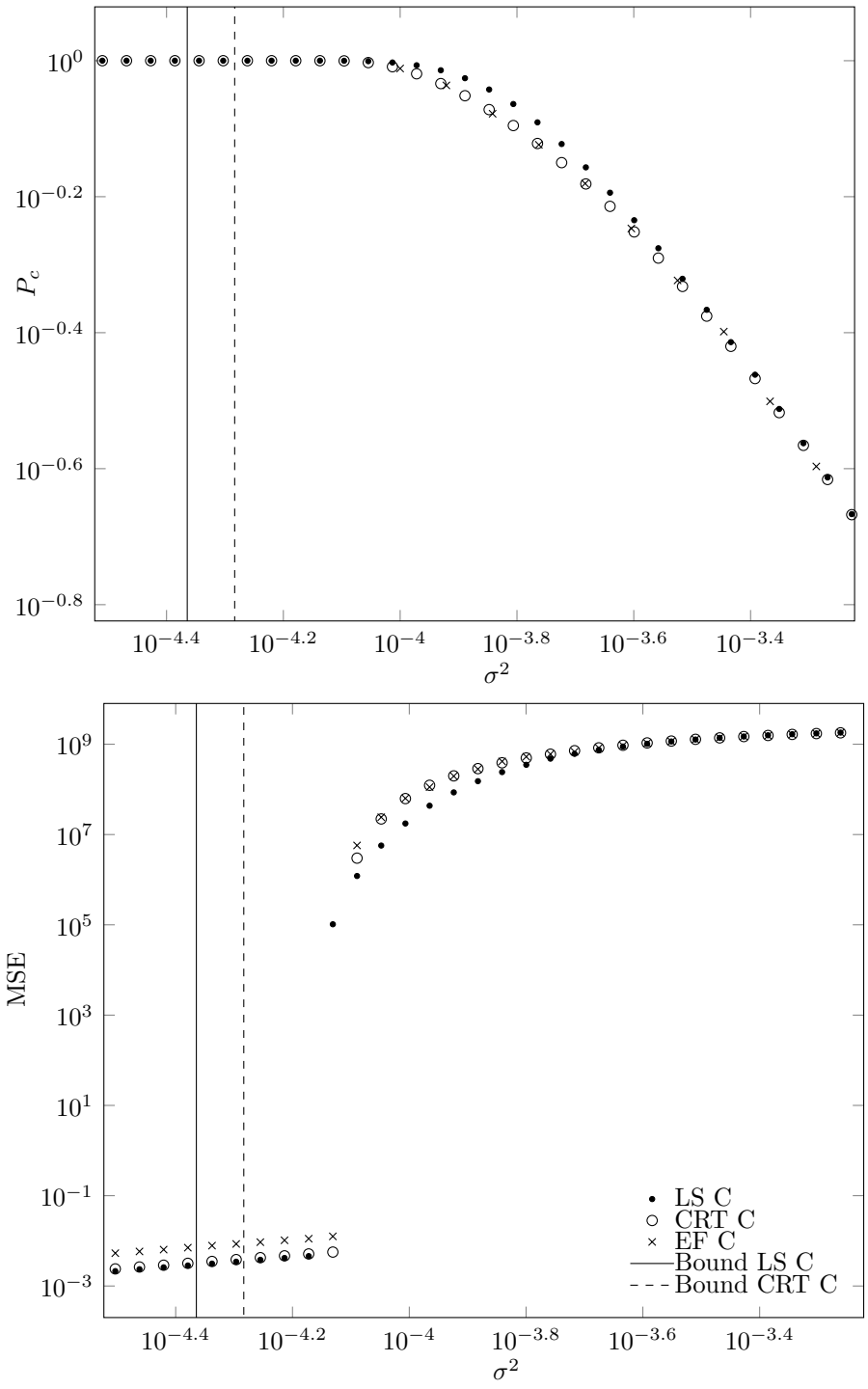

Figure 4.3: Probability of correct estimation of wrapping variables P_c (top), sample mean square error (MSE) (bottom), and bounds on variance with wavelengths C.

The true range in this example is $r_0 = 4000$ and the maximum measurable range is $\text{lcm}(C) = 83980$. For these wavelength the bounds

$$\tau_{\text{LS}} \approx 1.138 \times 10^{-2} \qquad \text{and} \qquad \tau_{\text{CRT}} \approx 1.25 \times 10^{-2}$$

to four significant figures. In this example, the probability of correctly estimating the wrapping variables for the least squares and the CRT estimator is almost the same. The probability $P_c = 1$ when $\sigma^2 < \tau_{\text{LS}}^2/3 \approx 4.319 \times 10^{-5}$ for the least squares range estimator and when $\sigma^2 < \tau_{\text{CRT}}^2/3 \approx 5.208 \times 10^{-5}$ for the CRT estimator. The mean square error plot on the bottom of Figure 4.3 shows that the CRT estimator performs slightly better in this case. This figure also shows results for the excess fractions method that performs similar to the CRT estimator.

We observe from simulation results that upper bound τ_{LS} on phase errors, probability P_c of correct wrapping variable estimation and mean square error depend on wavelengths used for range estimation. This leads to a natural question that whether it is possible to select wavelengths that improve these performance metrics. This is an interesting and nontrivial problem and is investigated in Chapter 5.

4.5 Summary

In this chapter, we provided a formal definition of correct wrapping variables and found that the wrapping variables for the least squares range estimator are correct whenever the projection of the phase noise is contained in the interior of the Voronoi cell of Λ^*. As the characterization of the phase noise in terms of the Voronoi cell of a lattice is not trivial, we instead used inradius of the lattice to define a condition for the correctness of the wrapping variables. Based on this condition we derive an upper bound for the least squares range estimator. We found that if all absolute phase measurement errors are less than this bound, then the least squares range estimator is guaranteed to correctly estimate the wrapping variables. We compared this with a similar bound derived for estimators based on the Chinese remainder theorem. The bound for the least squares estimator is often larger. This corroborates with existing empirical evidence suggesting

that the least squares estimator is often more accurate than those estimators based on the CRT.

The bound for the least squares range estimator derived in this chapter is based on the inradius of a lattice. The inradius depends upon the lattice which in turn depends upon the wavelengths. This naturally leads us to the question of whether it is possible to select wavelengths that maximise the inradius and hence the probability of correctness of these wrapping variables. This is an interesting and nontrivial problem that is investigated in Chapter 5.

Chapter 5

Wavelength Selection for Least Squares Estimation of Range

5.1 Introduction

We observed in previous chapters that the accuracy of the least squares range estimator is dependent upon the values of measurement wavelengths. However, the relationship between wavelengths and range estimation accuracy is nontrivial and this complicates wavelength selection procedures. In this chapter develop an algorithm to automatically select wavelengths for use with the least square range estimator from [34]. The wavelength selection procedure is typically subject to practical constraints such as minimum and maximum wavelength (i.e. bandwidth constraints) and constraints on the maximum identifiable range. Procedures have been described for the beat wavelength method [18] and for the method of excess fractions [21]. Some of these methods are heuristic and require a non-negligible amount of experimentation. Procedures for selecting wavelengths for the CRT and least squares range estimators have not yet been developed.

For the least squares estimator one possible approach for wavelength selection is to utilise the inradius of the lattice. However, the relation between the measurement wavelengths and the inradius is also nontrivial. Therefore, in this chapter, we use the

relation between the wavelengths, the determinant of the lattice and its Voronoi cell to select wavelengths that maximise the accuracy of the estimator. We will notice that finding the determinant of a lattice using Corollary 1 is simple in our case that simplifies the wavelengths selection procedure for the least squares range estimator.

For the purpose of wavelengths selection, we devise an optimisation criterion connected with the mean square error under constraints on the minimum and maximum wavelengths and on the identifiable range. The optimisation criterion is developed using the interesting properties of a particular class of *lattices*, a structure common in algebraic and computational number theory [36, 37, 62, 68]. These properties lead to simple and sufficiently accurate approximations for the mean square range error in terms of the wavelengths. The resulting constrained optimisation problem is simple enough to be minimised by a depth first search. Monte-Carlo simulations indicate that wavelengths that minimise this criterion can result in considerably more accurate range estimates than wavelengths selected by ad hoc means.

The chapter is organised as follows. Section 5.2 provides an upper bound on the correct solution of the quadratic form (3.15) using a well known relation between the determinant of a lattice and it Voronoi cell. The interesting properties of a particular class of lattices constructed by intersection with and projection onto a subspace are described. These properties are used to develop simple and sufficiently accurate approximations for the mean square error of the least squares range estimator in Section 5.3. Section 5.4 uses these approximations to design an optimisation criterion related to the mean square error and describes an algorithm to compute wavelengths that minimise the criterion. The algorithm is based on depth first search and can take a long time when the number of wavelength is not small. For this case we describe two methods that reduce the search time at the expense of not guaranteeing that the true minimising wavelengths are found. The results of Monte-Carlo simulations are presented in Section 5.5. The simulations indicate that wavelengths that minimise (or approximately minimise) the criterion can result is considerably more accurate range estimates than wavelengths selected by ad hoc means. The simulations corroborate

with existing empirical evidence suggesting that the least squares range estimator is often more accurate than other estimators [34, 69].

5.2 Bound on the Correctness of Wrapping Variables

In this section we utilise the concepts introduced in Section 4.2. To motivate our wavelength selection procedure we make the assumption that the phase noise $\Phi_1, \ldots, \Phi_n$ in (4.1) are zero mean, independent and identically distributed (i.i.d.) wrapped normal random variables [61, p. 50][62, p. 76][17, p. 47]. In this case,

$$\Phi_n = \langle \epsilon_n \rangle \qquad n = 1, \ldots, N$$

where $\epsilon_1, \ldots, \epsilon_N$ are independent and identically distributed normal random variables with zero mean and variance σ^2. Under this assumption, the least squares range estimator from [34] is also the maximum likelihood estimator. Observe that

$$Y = \langle r_0/\lambda_n + \Phi_n \rangle = \langle r_0/\lambda_n + \langle \epsilon_n \rangle \rangle = \langle r_0/\lambda_n + \epsilon_n \rangle$$

and that the phase differences can be written in the form

$$Y_n = \langle r_0/\lambda_n + \epsilon_n \rangle = r_0/\lambda_n + \epsilon_n + \zeta_n$$

where the integers

$$\zeta_n = -\lceil r_0/\lambda_n + \epsilon_n \rfloor \qquad n = 1, \ldots, N$$

are called *wrapping variables*. The wrapping variables are related to the number of whole wavelengths that occur over the range r_0 between the transmitter and the receiver. Writing in column vector form

$$\mathbf{y} = r_0\mathbf{w} + \boldsymbol{\epsilon} + \boldsymbol{\zeta} \tag{5.1}$$

where the column vectors

$$\mathbf{y} = \begin{pmatrix} Y_1 \\ \vdots \\ Y_N \end{pmatrix} \quad \boldsymbol{\zeta} = \begin{pmatrix} \zeta_1 \\ \vdots \\ \zeta_N \end{pmatrix} \quad \mathbf{w} = \begin{pmatrix} \frac{1}{\lambda_1} \\ \vdots \\ \frac{1}{\lambda_N} \end{pmatrix} \quad \boldsymbol{\epsilon} = \begin{pmatrix} \epsilon_1 \\ \vdots \\ \epsilon_N \end{pmatrix}.$$

It is shown in Section 3.3, that the least squares estimator $\hat{\boldsymbol{\zeta}} \in \mathbb{Z}^N$ of the wrapping variables minimises the quadratic form

$$\|\mathbf{Q}\mathbf{y} - \mathbf{Q}\mathbf{z}\|^2 \qquad \text{over } \mathbf{z} \in \mathbb{Z}^N, \tag{5.2}$$

where $\|\cdot\|$ indicates the Euclidean norm of a vector. Given $\hat{\boldsymbol{\zeta}}$, the least square range estimator $\hat{r}$ is then given by (4.2). It is shown in Section 3.3 how the quadratic form (5.2) can be minimised over $\mathbb{Z}^N$ by computing a closest point in a *lattice*. We will use the properties of this lattice from Section 2.1 to develop our wavelength selection procedure.

Of interest to us is the probability that an m-variate normal random variable with i.i.d. components having zero mean and variance σ^2 lies inside the Voronoi cell. We denote this probability by

$$P(\Lambda, \sigma^2) = \frac{1}{\sigma^m \sqrt{(2\pi)^m}} \int_{\text{Vor}\,\Lambda} e^{-\|\mathbf{x}\|^2/2\sigma^2} d\mathbf{x}. \tag{5.3}$$

This probability can be upper bounded by the probability that an n-variate normal random variable lies within a sphere of n-volume equal to the determinant of the lattice $\det\Lambda$ using (2.1), i.e.,

$$P(\Lambda, \sigma^2) \leq F_n\left(\frac{\Gamma(n/2+1)^{2/n}(\det\Lambda)^{2/n}}{\pi\sigma^2}\right) \tag{5.4}$$

where F_n is the chi-square cumulative distribution function with n degrees of freedom and Γ is the gamma function. This upper bound will be involved in the construction of our wavelength optimisation criterion in Section 5.4. The probability $P(\Lambda, \sigma^2)$ can be lower bounded by the probability that an n-variate normal random variable lies within

a sphere of radius equal to the inradius ρ of the lattice, i.e.,

$$P(\Lambda, \sigma^2) \geq F_n(\rho/\sigma^2). \tag{5.5}$$

It may be possible to build an alternative wavelength optimisation criterion using this lower bound rather than (5.4). However, the relationship between the wavelengths and the inradius ρ is nontrivial and so we have not attempted this here.

Recall from (5.2) that the least squares range estimator first computes an estimate $\hat{\boldsymbol{\zeta}} \in \mathbb{Z}^N$ of the wrapping variables by minimising the quadratic form $\|\mathbf{Qy} - \mathbf{Qz}\|^2$ with respect to $\mathbf{z} \in \mathbb{Z}^N$. Recall from Section 4.2 that the $N \times N$ matrix $\mathbf{Q}$ is the orthogonal projection into the $N-1$ dimensional subspace orthogonal to the vector $\mathbf{w}$ containing the reciprocals of the wavelengths (4.3). Let H denote this subspace. The elements in the vector $\mathbf{v} = P\mathbf{w}$ are jointly relatively prime and so, by Corollary 1, the set $\Lambda = \mathbb{Z}^N \cap H$ is an $N-1$ dimensional lattice with determinant $\det \Lambda = \|\mathbf{v}\|$ and dual lattice $\Lambda^* = \{\mathbf{Qz} \ ; \ \mathbf{z} \in \mathbb{Z}^N\}$. We see that the problem of minimising the quadratic form (5.2) is precisely that of finding a closest lattice point to $\mathbf{Qy}$ in the lattice Λ^*.

This connection between the least squares range estimator and the closest lattice point problem appears to have been first realised by Teunissen [4]. In Section 4.2 we defined the concept of correct wrapping variables. In the next section, using the definition of correct wrapping variables, we will show that the least squares estimator $\hat{\boldsymbol{\zeta}}$ of the wrapping variables is correct when the noise $\boldsymbol{\epsilon}$ is contained within the Voronoi cell of the lattice Λ^*. This fact has been realised by numerous authors including Hassibi and Boyd [32] who relate it to what they call the problem of *verification*. More recently this has been utilised by Li et al. [33] and Akhlaq et al. [69] for studying the accuracy of the least squares range estimator.

The existing literature typically makes use of either the lower bound (5.5) based on the inradius ρ of the lattice Λ^* or the upper bound (5.4) based on the determinant $\det \Lambda^*$. The relationship between the wavelengths and the inradius is non trivial. So far in the literature $\det \Lambda^*$ has been computed by first finding a basis matrix $\mathbf{B}$ for the lattice Λ^* and then computing the determinant directly as $\det \Lambda^* = \sqrt{\det \mathbf{B}'\mathbf{B}}$.

The relationship between the wavelengths and the basis $\mathbf{B}$ is nontrivial [34] and the determinant of the $N \times N$ matrix $\mathbf{B}'\mathbf{B}$ is also not given by a simple expression when N is not small. For these reasons it at first appears that the relationship between the wavelengths and the determinant $\det \Lambda^*$ is non trivial.

A key realisation we make in this thesis is that $\det \Lambda^*$ is related to the wavelengths in a simple way by Corollary 1. This corollary and the fact that $\det \Lambda^* = (\det \Lambda)^{-1}$ shows that $\det \Lambda^*$ takes the simple form

$$\det \Lambda^* = \frac{1}{\|\mathbf{v}\|} = \frac{1}{\|P\mathbf{w}\|} = \frac{1}{P\sqrt{\sum_{i=1}^{N} \lambda_i^{-2}}}.$$

Combining this simple expression with the upper bound (5.4) will lead to a simple and sufficiently accurate approximation of the probability that the least square estimator of the unwrapping variables is correct, that is, an approximation of the probability that $\mathbf{Q}\hat{\boldsymbol{\zeta}} = \mathbf{Q}\boldsymbol{\zeta}$. It is this simple approximation that leads to our optimisation criterion for selecting wavelengths.

5.3 Approximating range error

In Section 5.4 we will describe a procedure for selecting favourable sets of wavelengths for the least squares range estimator. To do so, we first require approximations for the error of the range estimator in terms of the wavelengths $\lambda_1, \ldots, \lambda_N$. We consider two approximations. The first approximates the error in the case that the least squares estimator of the wrapping variables $\hat{\boldsymbol{\zeta}}$ is correct. The second uses (5.4) to upper bound the probability that $\hat{\boldsymbol{\zeta}}$ is correct.

Recall from Section 4.2 that when the wrapping variables are correct $\mathbf{Q}\hat{\boldsymbol{\zeta}} = \mathbf{Q}\boldsymbol{\zeta}$ or equivalently $\boldsymbol{\zeta} = \hat{\boldsymbol{\zeta}} + kP\mathbf{w}$ for some $k \in \mathbb{Z}$. In this case, the least squares estimator of the range takes the form (4.2),

$$\hat{r} = \frac{(\mathbf{y} - \hat{\boldsymbol{\zeta}})'\mathbf{w}}{\mathbf{w}'\mathbf{w}} = \frac{(\mathbf{y} - \boldsymbol{\zeta} + kP\mathbf{w})'\mathbf{w}}{\|\mathbf{w}\|^2}.$$

Substituting (5.1) for $\mathbf{y}$ we find that

$$\hat{r} = \frac{\boldsymbol{\epsilon}'\mathbf{w}}{\|\mathbf{w}\|^2} + r_0 + kP.$$

Recall from Section 4.2 that range estimates $\hat{r}$ and $\hat{r}+kP$ are considered equivalent for integers k. For this reason the error of the least squares range estimator corresponds with the term $\boldsymbol{\epsilon}'\mathbf{w}/\|\mathbf{w}\|^2$. Under our assumption that $\epsilon_1, \ldots, \epsilon_N$ are i.i.d. and normally distributed with zero mean and variance σ^2 this error is normally distributed with zero mean and variance

$$\operatorname{var} \frac{\boldsymbol{\epsilon}'\mathbf{w}}{\|\mathbf{w}\|^2} = \frac{\sigma^2}{\|\mathbf{w}\|^2} = \frac{\sigma^2}{\sum_{n=1}^{N} \lambda_n^{-2}}. \tag{5.6}$$

The variance decreases as $\sum_{n=1}^{N} \lambda_n^{-2}$ increases. The variance (5.6) serves as an approximation of the mean square error of the least squares range estimator when the estimated wrapping variables $\hat{\boldsymbol{\zeta}}$ are correct. The simulation results in Section 5.5 suggest this approximation to be very close.

We now approximate the probability that the wrapping variables are correct, that is, we approximate the probability that $\mathbf{Q}\hat{\boldsymbol{\zeta}} = \mathbf{Q}\boldsymbol{\zeta}$. Our approximation is based upon the upper bound (5.4). Recall that $\hat{\boldsymbol{\zeta}}$ minimises the quadratic form $\|\mathbf{Q}\mathbf{y} - \mathbf{Q}\mathbf{z}\|^2$ over $\mathbf{z} \in \mathbb{Z}^N$. It follows that $\mathbf{Q}\hat{\boldsymbol{\zeta}}$ is a closest point in the lattice $\Lambda^* = \{\mathbf{Q}\mathbf{z}\ ;\ \mathbf{z} \in \mathbb{Z}^N\}$ to the point $\mathbf{Q}\mathbf{y}$. Equivalently,

$$\mathbf{Q}\mathbf{y} - \mathbf{Q}\hat{\boldsymbol{\zeta}} \in \operatorname{Vor} \Lambda^*$$

from the definition of the Voronoi cell. Using (5.1),

$$\mathbf{Q}\mathbf{y} - \mathbf{Q}\hat{\boldsymbol{\zeta}} = \mathbf{Q}(r_0\mathbf{w} + \boldsymbol{\epsilon} + \boldsymbol{\zeta}) - \mathbf{Q}\hat{\boldsymbol{\zeta}} = \mathbf{Q}\boldsymbol{\epsilon} - \mathbf{Q}(\hat{\boldsymbol{\zeta}} - \boldsymbol{\zeta})$$

and so

$$\mathbf{Q}\boldsymbol{\epsilon} - \mathbf{Q}(\hat{\boldsymbol{\zeta}} - \boldsymbol{\zeta}) \in \operatorname{Vor} \Lambda^*.$$

We see that $\mathbf{Q}(\boldsymbol{\zeta} - \hat{\boldsymbol{\zeta}})$ is a closest lattice point to the projection of the noise variables $\mathbf{Q}\boldsymbol{\epsilon}$. If $\mathbf{Q}\boldsymbol{\epsilon}$ lies in the interior of the $\operatorname{Vor} \Lambda^*$ then the unique closest lattice point is the origin $\mathbf{0}$, that is, $\mathbf{Q}(\boldsymbol{\zeta} - \hat{\boldsymbol{\zeta}}) = \mathbf{0}$ or equivalently $\mathbf{Q}\boldsymbol{\zeta} = \mathbf{Q}\hat{\boldsymbol{\zeta}}$. We have found that the least square estimator $\hat{\boldsymbol{\zeta}}$ of the unwrapping variables is correct if the projection $\mathbf{Q}\boldsymbol{\epsilon}$ of the

noise variables lies within the interior of the Voronoi cell. The estimator $\hat{\boldsymbol{\zeta}}$ can similarly be shown to be incorrect if $\mathbf{Q}\boldsymbol{\epsilon} \notin \operatorname{Vor}\Lambda^*$. Because the boundary of the Voronoi cell has zero n-volume, it follows that the probability the unwrapping variables are correct is the same as the probability that $\mathbf{Q}\boldsymbol{\epsilon}$ lies in $\operatorname{Vor}\Lambda^*$

A further simplification can be made. The $N-1$ dimensional lattice Λ^* lies in the subspace orthogonal to $\mathbf{w}$ and so $\operatorname{Vor}\Lambda^*$ is unbounded in the direction of $\mathbf{w}$. Specifically, $\mathbf{Q}\boldsymbol{\epsilon} \in \operatorname{Vor}\Lambda^*$ if and only if $\mathbf{Q}\boldsymbol{\epsilon} + s\mathbf{w} \in \operatorname{Vor}\Lambda^*$ for all $s \in \mathbb{R}$. Because $\boldsymbol{\epsilon} = \mathbf{Q}\boldsymbol{\epsilon} + s\mathbf{w}$ for some s, it follows that $\mathbf{Q}\boldsymbol{\epsilon} \in \operatorname{Vor}\Lambda^*$ if and only if $\mathbf{Q}\boldsymbol{\epsilon} + s\mathbf{w} = \boldsymbol{\epsilon} \in \operatorname{Vor}\Lambda^*$, that is,

$$\mathbf{Q}\boldsymbol{\epsilon} \in \operatorname{Vor}\Lambda^* \Leftrightarrow \boldsymbol{\epsilon} \in \operatorname{Vor}\Lambda^*.$$

Thus, the probability that the unwrapping variables are correct is the same as the probability that the noise $\boldsymbol{\epsilon}$ lies in $\operatorname{Vor}\Lambda^*$, that is, the same as the probability $P(\Lambda^*, \sigma^2)$ from (5.3). We approximate this probability by the upper bound (5.4),

$$P(\Lambda^*, \sigma^2) \leq F_{N-1}\left(\frac{\Gamma\left(\frac{N}{2}+\frac{1}{2}\right)^{2/(N-1)}}{\|\mathbf{v}\|^{2/(N-1)}\sigma^2\pi}\right) \tag{5.7}$$

where we have used the simple expression $\det\Lambda^* = \|\mathbf{v}\|^{-1}$ derived from Corollary 1. This bound depends upon the wavelengths $\lambda_1, \ldots, \lambda_N$ only through the term

$$\|\mathbf{v}\|^2 = \|P\mathbf{w}\|^2 = P^2\sum_{n=1}^{N}\lambda_n^{-2} = \operatorname{lcm}^2(\lambda_1, \ldots, \lambda_N)\sum_{n=1}^{N}\lambda_n^{-2}.$$

The bound increases as this term decreases.

This bound (5.7) for the probability of correct unwrapping is simpler than similar bounds in the literature that involve computing the determinant $\det\Lambda^* = \sqrt{\det\mathbf{B}'\mathbf{B}}$ directly [32, 33]. The simplicity of our bound is made possible by Corollary 1 leading to the simple expression $\det\Lambda^* = \|\mathbf{v}\|^{-1}$. This simplicity enables the wavelength selection procedure we describe in the next section.

5.4 Selecting wavelengths for range estimation

In the previous section two approximations, (5.6) and (5.7), related to range error were developed. The first approximation (5.6) describes the variance of the range error when the wrapping variables are correct. To decrease this variance we should choose wavelengths such that

$$\frac{\sigma^2}{\sum_{n=1}^{N} \lambda_n^{-2}}$$

is small. The second approximation (5.7) upper bounds the probability that the wrapping variables are correct. To increase this bound we should choose wavelengths such that

$$P^2 \sum_{n=1}^{N} \lambda_n^{-2} = \mathrm{lcm}^2(\lambda_1, \ldots, \lambda_N) \sum_{n=1}^{N} \lambda_n^{-2}$$

is small.

These are two competing objectives. To have both small estimator variance while simultaneously allowing large probability of correct unwrapping we propose to choose wavelengths that minimise an objective function of the form

$$L(\lambda_1, \ldots, \lambda_N) = P^2 \sum_{n=1}^{N} \lambda_n^{-2} + \frac{\gamma}{\sum_{n=1}^{N} \lambda_n^{-2}} \tag{5.8}$$

where $\gamma > 0$ weights the importance of the individual objectives and is free to be chosen. The weight γ can be chosen to incorporate σ^2 if it is known. We have found that choosing

$$\gamma = \frac{N^2 r_{\max}^2}{\lambda_{\max}^2 \lambda_{\min}^2}$$

works well empirically. The quantities $r_{\max}$, $\lambda_{\min}$, and $\lambda_{\max}$ will be introduced shortly. This choice for γ is used in the experiments performed in Section 5.5 and has the convenient property of being independent of the noise variance σ^2. The choice is approximately the ratio of the minimum value of the two individual objectives. The motivation behind this being to approximately balance the importance given to both objectives.

We incorporate into this optimisation problem three practical constraints. First, we suppose that the wavelengths are all contained in an interval $[\lambda_{\min}, \lambda_{\max}]$. In practice the minimum and maximum allowable wavelengths $\lambda_{\min}$ and $\lambda_{\max}$ might be dictated by hardware constraints, such as antennae size, or properties of the medium through which the signal propagates. The second constraint is upon the maximum identifiable range. We suppose that the system must be capable of unambiguously estimating range on an interval of some prespecified length $r_{\max}$, that is, $P \geq r_{\max}$. For example $r_{\max}$ maybe a few meters for indoor applications, a few tens of meters for outdoor electronic surveying, and a few thousand kilometers for global positioning via satellite. Finally, we assume that one of the wavelengths, say λ_1, is fixed and known. We assume that $\lambda_1 = \lambda_{\max}$ in what follows. This constraint simplifies the optimisation problem and, since $\lambda_{\max}$ is free to be selected, results in only minor loss of generality.

Our optimisation problem is now to find wavelengths $\lambda_2, \ldots, \lambda_N$ that minimise

$$L_1(\lambda_2, \ldots, \lambda_N) = L(\lambda_{\max}, \lambda_2, \ldots, \lambda_N)$$

subject to constraints

$$\lambda_{\min} \leq \lambda_n \leq \lambda_{\max} \qquad n = 2, \ldots, N \tag{5.9}$$

$$P = \operatorname{lcm}(\lambda_{\max}, \lambda_2, \ldots, \lambda_N) \geq r_{\max}. \tag{5.10}$$

These are referred to as the *bandwidth constraint* and the *range constraint* respectively. The least common multiple $P = \operatorname{lcm}(\lambda_{\max}, \lambda_2, \ldots, \lambda_N)$ depends upon the wavelengths in a non trivial way. This optimisation problem is multivariate, nonlinear, and non-convex with nonconvex constraints. It is not immediately obvious how a solution is to be found. We will show how this problem can be transformed into an equivalent problem involving $2(N-1)$ integer parameters. This equivalent problem can be solved by a depth first search.

A solution of the minimisation problem is such that the wavelengths $\lambda_1 = \lambda_{\max}$ and $\lambda_2, \ldots, \lambda_{N-1}$ are rationally related, that is, λ_n/λ_m is rational for all n, m. Otherwise, $P = \operatorname{lcm}(\lambda_{\max}, \lambda_2, \ldots, \lambda_N) = \infty$ and L_1 will not be minimised. Thus, there exist

positive integers $p_2, \ldots, p_N$ and $q_2, \ldots, q_N$ such that $\gcd(p_n, q_n) = 1$ and

$$\lambda_n = \frac{p_n}{q_n}\lambda_1 = \frac{p_n}{q_n}\lambda_{\max} \qquad n = 2, \ldots, N. \tag{5.11}$$

Now,

$$P = \operatorname{lcm}\left(\lambda_{\max}, \frac{p_2}{q_2}\lambda_{\max}, \ldots, \frac{p_N}{q_N}\lambda_{\max}\right) = \lambda_{\max} Q \tag{5.12}$$

where

$$Q = \operatorname{lcm}\left(1, \frac{p_2}{q_2}, \ldots, \frac{p_N}{q_N}\right).$$

A simpler expression for Q can be obtained. Let $\ell_1, \ldots, \ell_N$ satisfy

$$\ell_1 = 1, \qquad \ell_n = \operatorname{lcm}\left(\ell_{n-1}, \frac{p_n}{q_n}\right) \qquad n = 2, \ldots, N$$

and observe that $Q = \ell_N$. Because ℓ_1 is an integer and p_2 and q_2 are relatively prime $\ell_2 = \operatorname{lcm}(\ell_1, p_2/q_2) = \operatorname{lcm}(1, p_2)$ is an integer. Similarly,

$$\ell_3 = \operatorname{lcm}\left(\ell_2, \frac{p_3}{q_3}\right) = \operatorname{lcm}(\ell_2, p_3) = \operatorname{lcm}(1, p_2, p_3)$$

is an integer and, by induction,

$$\ell_N = \operatorname{lcm}\left(\ell_{N-1}, \frac{p_N}{q_N}\right) = \operatorname{lcm}(1, p_2, \ldots, p_N).$$

Now $Q = \ell_N = \operatorname{lcm}(p_2, \ldots, p_N)$. Observe that Q does not depend on the denominators $q_2, \ldots, q_N$. It is convenient to introduce vectors $\mathbf{p} = (p_2, \ldots, p_N)$ and $\mathbf{q} = (q_2, \ldots, q_N)$ and write $Q(\mathbf{p})$ to highlight the dependence of Q on $p_2, \ldots, p_N$.

From the range constraint (5.10) and (5.12),

$$Q(\mathbf{p}) = \operatorname{lcm}(p_2, \ldots, p_N) = \frac{P}{\lambda_{\max}} \geq \frac{r_{\max}}{\lambda_{\max}} \tag{5.13}$$

and from the bandwidth constraint (5.9) and (5.11),

$$\frac{\lambda_{\min}}{\lambda_{\max}} \leq \frac{p_n}{q_n} \leq 1 \qquad n = 2, \ldots, N. \tag{5.14}$$

Define the objective function

$$\begin{aligned} L_2(\mathbf{p},\mathbf{q}) &= L_1\big(\tfrac{p_2}{q_2}\lambda_{\max},\ldots,\tfrac{p_N}{q_N}\lambda_{\max}\big) \\ &= Q^2(\mathbf{p})D(\mathbf{p},\mathbf{q}) + \frac{\gamma\lambda_{\max}^2}{D(\mathbf{p},\mathbf{q})}. \end{aligned} \tag{5.15}$$

where

$$D(\mathbf{p},\mathbf{q}) = 1 + \sum_{n=2}^{N} \frac{q_n^2}{p_n^2}. \tag{5.16}$$

Our optimisation problem can now be re-encoded into that of finding integers vectors

$$\hat{\mathbf{p}} = (\hat{p}_2,\ldots,\hat{p}_N), \qquad \hat{\mathbf{q}} = (\hat{q}_2,\ldots,\hat{q}_N)$$

that minimise L_2 subject to constraints (5.13) and (5.14). Given these minimisers, the wavelengths

$$\hat{\lambda}_n = \frac{\hat{p}_n}{\hat{q}_n}\lambda_{\max} \qquad n = 2,\ldots,N$$

are a solution of the original optimisation problem, that is, these wavelengths minimise L_1 subject to the bandwidth and range constraints (5.9) and (5.10). We now describe an algorithm to find minimisers $\hat{\mathbf{p}}$ and $\hat{\mathbf{q}}$.

We first discover some bounds that the minimisers $\hat{p}_n, \hat{q}_n$ must satisfy. From (5.14) and (5.16),

$$N \le D(\hat{\mathbf{p}},\hat{\mathbf{q}}) \le 1 + \frac{(N-1)\lambda_{\max}^2}{\lambda_{\min}^2}. \tag{5.17}$$

Also

$$Q(\hat{\mathbf{p}}) = \operatorname{lcm}(\hat{p}_2,\ldots,\hat{p}_N) \ge \hat{p}_n \qquad n = 2,\ldots,N. \tag{5.18}$$

Let $\widehat{L} = L_2(\hat{\mathbf{p}},\hat{\mathbf{q}})$ be the minimum value of L_2 (and also of L_1) and let $\widetilde{L}$ be a finite upper bound on $\widehat{L}$. For example, it suffices to choose

$$\widetilde{L} = L_1\big(\tfrac{w}{w+1}\lambda_{\max},\ldots,\tfrac{w}{w+1}\lambda_{\max}\big) \tag{5.19}$$

where w is the smallest integer greater than or equal to both $r_{\max}/\lambda_{\max}$ and $\lambda_{\min}/(\lambda_{\max}-\lambda_{\min})$. With this choice $\frac{w}{w+1}\lambda_{\max} \in [\lambda_{\min},\lambda_{\max}]$ so that the bandwidth constraint is

satisfied and

$$\operatorname{lcm}\left(\lambda_{\max}, \tfrac{w}{w+1}\lambda_{\max}, \ldots, \tfrac{w}{w+1}\lambda_{\max}\right) = \lambda_{\max} w \geq r_{\min}$$

so that the range constraint is satisfied. Now,

$$\widetilde{L} \geq \widehat{L} = Q(\hat{\mathbf{p}})^2 D(\hat{\mathbf{p}}, \hat{\mathbf{q}}) + \frac{\gamma \lambda_{\max}^2}{D(\hat{\mathbf{p}}, \hat{\mathbf{q}})}$$

and using the inequalities (5.18) for $Q(\hat{\mathbf{p}})$ and (5.17) for $D(\hat{\mathbf{p}}, \hat{\mathbf{q}})$ we find that,

$$\widetilde{L} \geq \widehat{L} \geq \hat{p}_n^2 N + \gamma B \qquad \text{for all } n = 2, \ldots, N$$

where

$$B = \frac{\lambda_{\min}^2 \lambda_{\max}^2}{\lambda_{\min}^2 + (N-1)\lambda_{\max}^2}.$$

Because $\hat{p}_n \geq 1$ is a positive integer we obtain the following lower and upper bounds

$$1 \leq \hat{p}_n \leq \sqrt{\frac{\widetilde{L} - \gamma B}{N}} \qquad n = 2, \ldots, N. \tag{5.20}$$

Given $\hat{p}_n$ upper and lower bounds on $\hat{q}_n$ derive from the bandwidth constraint (5.14),

$$\hat{p}_n \leq \hat{q}_n \leq \frac{\lambda_{\max}}{\lambda_{\min}} \hat{p}_n \qquad n = 2, \ldots, N. \tag{5.21}$$

data To find minimisers of L_2, it suffices to check only those integer vectors $\hat{\mathbf{p}}$ and $\hat{\mathbf{q}}$ with elements satisfying the above two inequalities (5.20) and (5.21). Because the number of integer vectors satisfying these inequalities is finite this procedure will terminate in finite time. The number of candidate solutions that need to be checked can be reduced by incorporating the property $\gcd(\hat{p}_n, \hat{q}_n) = 1$ into the search. The number of candidates is further reduced by noting that the objective function L_1 is unchanged by permutation of the wavelengths $\lambda_2, \ldots, \lambda_N$. Equivalently, $L_2(\mathbf{p}, \mathbf{q})$ is unchanged if both arguments $\mathbf{p}$ and $\mathbf{q}$ undergo the same permutation. For this reason it is sufficient to suppose that the elements of $\hat{\mathbf{p}}$ are in, say, ascending order, that is, $\hat{p}_2 \leq \hat{p}_3 \leq \cdots \leq \hat{p}_N$.

Psuedocode describing the search procedure is given in Algorithm 1. The algorithm makes use of two functions psearch and qsearch that are called recursively. The integer variables N, $p_2, \ldots, p_N$, $q_2, \ldots, q_N$, and the real variables $\widetilde{L}, \gamma, B$ are assumed to be globally accessible to both functions psearch and qsearch. The while loop on line 1 of psearch iterates over those p_n satisfying (5.20). The while loop on line 1 of qsearch iterates over those q_n satisfying (5.21). The condition on line 2 of qsearch ensures that only those relatively prime p_n, q_n are included in the search. Lines 6 to 8 update the minimum found value of the objective function $\tilde{L}$ and the corresponding wavelengths whenever a new minimiser of the objective function L_2 is found.

This depth first search becomes computationally expensive if the number of wavelengths is not small or the minimum range $r_{\max}$ is large when compared with the maximum wavelength $\lambda_{\max}$. For this reason we now suggest some methods that accelerate the search at the expense of not necessarily guaranteeing that the true minimisers of L are found. The first method simply terminates the search after a specified amount of time and takes the best wavelengths found to that point. This approach is simple, but can be highly effective because the minimisers of L are regularly found well before the search completes.

The second method places a more restrictive upper bound on $\hat{p}_2, \ldots, \hat{p}_N$. The upper bound is motivated by physical constraints regularly occurring in practice that limit the accuracy to which a signal of a given wavelength can be generated [23, Sec. 5.B]. Rather than the upper bound from (5.20) a smaller fixed constant, say κ, is chosen and those p_n satisfying $1 \leq \hat{p}_n \leq \kappa$ are searched. The condition on Line 1 of psearch is correspondingly modified to $p_n \leq \kappa$. From (5.21) we see that the new bound on $\hat{p}_n$ places a new bound on $\hat{q}_n$,

$$\hat{q}_n \leq \frac{\lambda_{\max}}{\lambda_{\min}} \hat{p}_n \leq \frac{\lambda_{\max}}{\lambda_{\min}} \kappa$$

Recall that the wavelengths take the form $\hat{\lambda}_n = \hat{p}_n \lambda_{\max} / \hat{q}_n$ and so this new bound limits the resolution of the wavelengths searched by the optimiser. Specifically, the wavelengths are restricted to the form $\lambda_{\max} p/q$ where $p \leq q$ and q is smaller than $\kappa \lambda_{\max} / \lambda_{\min}$.

In practice we cannot generate sinusoidal signals with arbitrarily precise wavelengths. For example, optical interferometric experiments are limited by uncertainties in the refractive index of the medium through which the signal propagates [23, Sec. 5.B]. Audio and radio frequency devices are limited by the stability of oscillators used to generate signals. For these reasons, restricting the wavelength optimisation to a finite resolution is likely to be of little practical consequence. It might even be necessary for some applications. In practice, one might select κ so that $\kappa\lambda_{\max}/\lambda_{\min}$ is related to the precision with which a sinusoidal signal can be generated.

Algorithm 1 Computes wavelengths optimised for the least squares range estimator.

Input: $N, r_{\max}, \lambda_{\min}, \lambda_{\max}, \gamma$

1 $d = \lceil \max\left(\frac{r_{\max}}{\lambda_{\max}}, \frac{\lambda_{\min}}{\lambda_{\max}-\lambda_{\min}}\right)\rceil$ $(\hat{\lambda}_2, \ldots, \hat{\lambda}_N) = \left(\frac{w}{w+1}\lambda_{\max}, \ldots, \frac{w}{w+1}\lambda_{\max}\right)$ $\widetilde{L} = L_1\left(\hat{\lambda}_2, \ldots, \hat{\lambda}_N\right)$ $B = \frac{\gamma\lambda_{\min}^2\lambda_{\max}^2}{\lambda_{\min}^2+(N-1)\lambda_{\max}^2}$ $p_2 = 1$ psearch(2) **return** $(\lambda_{max}, \hat{\lambda}_2, \ldots, \hat{\lambda}_N)$

Function psearch(n)

Input: $n \in \{2, \ldots, N\}$

1 **while** $p_n^2 \leq (\widetilde{L} - \gamma B)/N$ **do**
2 $q_n = p_n$
3 qsearch(n)
4 $p_n = p_n + 1$

Function qsearch(n)

Input: $n \in \{2, \ldots, N\}$

1 **while** $q_n \leq p_n\lambda_{max}/\lambda_{min}$ **do**
2 **if** $\gcd(p_n, q_n) = 1$ **then**
3 **if** $n < N$ **then**
4 $p_{n+1} = p_n$
5 psearch($n+1$)
6 **else if** $L_2(\mathbf{p}, \mathbf{q}) \leq \widetilde{L}$ and $\mathrm{lcm}(\mathbf{p}) \geq \frac{r_{max}}{\lambda_{max}}$ **then**
7 $\widetilde{L} = L_2(\mathbf{p}, \mathbf{q})$
8 $\hat{\lambda}_n = \lambda_{\max} p_n/q_n \;\; n = 2, \ldots, N$
9 $q_n = q_n + 1$

5.5 Simulation Results

We present the results of Monte-Carlo simulations with the least squares range estimator, the excess fractions estimator [20], the algebraic method of Falaggis et al. [23], and range estimators based on the single-stage and multi-stage CRT algorithms of Xiao et al. [31]. In each simulation the phase noise variables $\Phi_1, \ldots, \Phi_N$ are wrapped normally distributed, that is, $\Phi_n = \langle \epsilon_n \rangle$ where $\epsilon_1, \ldots, \epsilon_N$ are independent and normally distributed with zero mean and variance σ^2. The number of Monte-Carlo trials used for each value of σ^2 is 10^5.

Figure 5.1 shows the sample mean square error of these estimators for $N = 3$ wavelengths. In each simulation the true range is $r_0 = 6\pi$ and we consider two different sets of wavelengths

$$A = \{2, 3, 5\}, \qquad B = \{\tfrac{30}{13}, \tfrac{15}{4}, 5\}.$$

The wavelengths from both sets are contained in the interval $[2, 5]$ and the identifiable range is $\text{lcm}(A) = \text{lcm}(B) = 30$. The wavelengths A are used in the simulations of Li et. al. [33] and B are optimised wavelengths given by Algorithm 1. When the noise variance is small the probability that the wrapping variables are correct is large and so we expect the mean square error to be similar to ((5.6)). This predicted mean square error is shown by the solid line for wavelengths A and by the dashed line for wavelengths B. Observed from Figure 5.1 that these predictions accurately model the behaviour of the least squares estimator when σ^2 is small. Wavelengths A result in slightly reduced sample mean square error compared with B when σ^2 is small. As σ^2 increases the sample mean square error exhibits a threshold effect and increases suddenly. The threshold occurs at $\sigma^2 \approx 5 \times 10^{-4}$ for wavelengths A and $\sigma^2 \approx 9 \times 10^{-4}$ for wavelength B. Wavelengths B are more accurate than A when σ^2 is greater than approximately 5×10^{-4}. The threshold for the CRT and excess fractions based range estimators occurs at approximately the same value of σ^2 with wavelengths A. The CRT estimator performs poorly with wavelengths B. The threshold for the excess fractions estimator is similar to that of the least squares estimator with wavelength B. However,

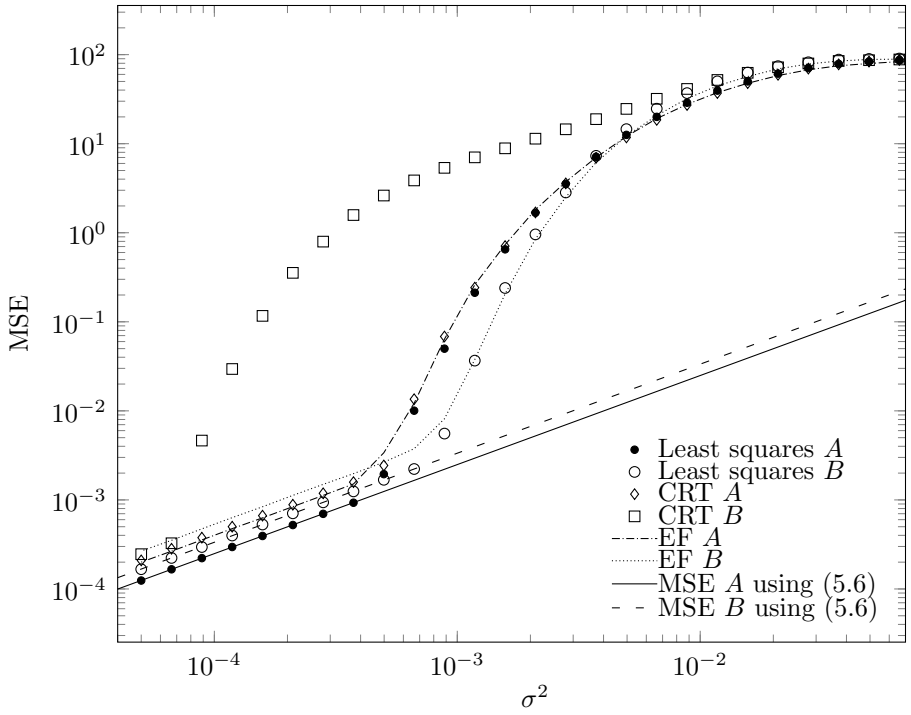

Figure 5.1: Sample mean square error of the least squares range estimator, the excess fraction based range estimator [20] and the range estimator based on the single stage and multi-stage CRT algorithms of Xiao et. al. [31] with $N = 3$ wavelenths.

the mean square error of the excess fraction estimator is larger than that of the least squares estimator when the noise variance is small.

Figure 5.3 displays the simulations results when there are $N = 4$ wavelengths from the sets

$$C = \{\tfrac{101039}{66}, \tfrac{1076285}{682}, \tfrac{198036440}{125389}, \tfrac{17572}{11}\},$$

$$D = \{1528, \tfrac{3868970284693}{25\times 10^8}, \tfrac{156953786407767}{10^{11}}, \tfrac{17572}{11}\}.$$

The wavelengths from both sets are contained in the interval $[1528, \frac{17572}{11}]$. Wavelengths D are those selected for the excess fractions estimator using the procedure described in [21]. These wavelengths are measured in nanometers in [21]. The least common multiple of D is greater than 2×10^{22} meters. However, the maximum range of the excess fractions estimator is not the least common multiple, but is instead what is called the *unambiguous measurement range* (UMR) [21] and is $1.8 \times 10^7 \text{nm} = 0.018\,\text{m}$ in this case. Wavelengths C are optimised for the least squares estimator using Algorithm 1 with $r_{\max} = 1.8 \times 10^7$. To speed up the search we put $\kappa = 1000$ as described

in Section 5.4. The identifiable range with wavelengths C is

$$\text{lcm}(C) = 198036440/11 \approx 18003312 > 1.8 \times 10^7.$$

In each simulation the true range $r_0 = 4000000\pi$. It can be observed from this figure that the single and multi-stage CRT estimators [31] and the algebraic method of Falaggis et al. [23] perform very poorly when compared with the excess fractions [20] and the least squares estimator. When σ^2 is less than $\approx 8 \times 10^{-6}$ the excess fractions based estimator performs slightly poor than the least squares estimator. As σ^2 increases the sample mean square error exhibits a threshold effect and increases suddenly. The threshold for the excess fractions and the least squares estimators occurs respectively at approximately 8×10^{-6} and 1.5×10^{-5}. The least squares estimator is more accurate than the excess fractions, the modified excess fractions and the single and multi-stage CRT estimators. It can also be observed that (5.6) provides a very good approximation for the MSE of the least squares estimator.

In another simulation in Figure 5.4 we compare the sample mean square error of the least squares range estimator, the excess fractions [20] and the single stage and multi-stage CRT based estimators of Xiao et. al. [31] with $N = 5$ wavelengths. In each simulation the true range $r_0 = 300\pi$. Two different sets of wavelengths are considered,

$$E = \{2, 3, 5, 7, 11\}, \quad F = \{\tfrac{22}{3}, \tfrac{66}{17}, \tfrac{77}{18}, \tfrac{110}{31}, 11\}.$$

The wavelengths from both sets are contained in the interval $[2, 11]$ and $P = \text{lcm}(E) = \text{lcm}(F) = 2310$ so that the identifiable range is the same. Wavelengths E are relatively prime integers and are used in [33]. Wavelengths F are obtained using Algorithm 1 with $\kappa = 15$.

The behaviour of the least squares, excess fractions and single-stage CRT estimators is similar for the wavelengths E. No benefit is gained by applying the multi-stage CRT estimator with wavelengths E. When the noise variance σ^2 is small the least squares estimator exhibits slightly smaller mean square error than the excess fractions and CRT estimators. As σ^2 increases the sample mean square error exhibits a

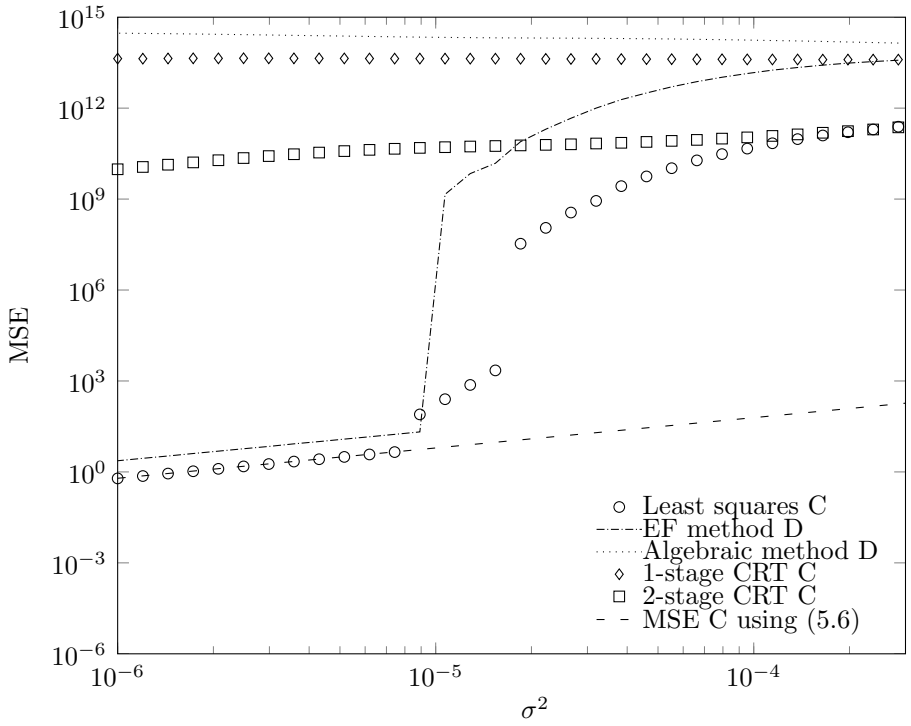

Figure 5.2: Sample mean square error of the least squares range estimator, the excess fraction based range estimator [20], the algebraic method of Falaggis et al. [23] and the range estimator based on the single stage and multi-stage CRT algorithms of Xiao et. al. [31] with $N = 4$ wavelenths.

'threshold' effect and increases suddenly. For wavelengths E this threshold occurs at $\sigma^2 \approx 8 \times 10^{-5}$.

Different behaviour is exhibited with wavelength F. When the noise variance σ^2 is small the least squares estimator exhibits slightly smaller mean square error with wavelengths E than with F. However, the threshold with wavelengths F occurs at $\sigma^2 \approx 2 \times 10^{-4}$. Wavelengths F are more accurate than E when σ^2 is greater than approximately 8×10^{-5}. The single-stage CRT estimator performs comparatively poorly with wavelengths F. A small improvement is gained by use of the multi-stage CRT estimator by splitting the wavelengths from F into two sets $\{\frac{110}{31}, 11\}$ and $\{\frac{22}{3}, \frac{66}{17}, \frac{77}{18}\}$. Simulations indicate that this is the best splitting of the wavelengths for the multi-stage CRT estimator in this case.

Figure 5.5 shows the computation time required for the least squares estimator computed using a sphere decoder, the single stage CRT estimator of Xiao et. al. [31] and the excess fractions based estimator [20] as the number of wavelengths N increases. The

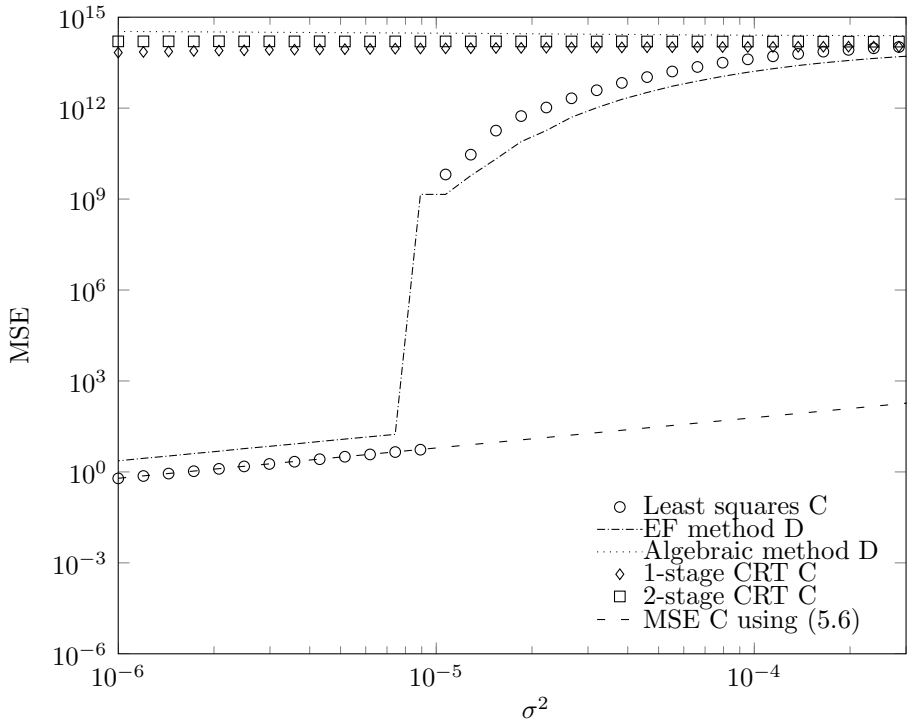

Figure 5.3: Sample mean square error of the least squares range estimator, the excess fraction based range estimator [20], the algebraic method of Falaggis et al. [23] and the range estimator based on the single stage and multi-stage CRT algorithms of Xiao et. al. [31] with $N = 4$ wavelenths.

wavelengths are set to integers $\{1, 2, 3, \ldots, N\}$ in each benchmark. In these benchmarks the least squares estimator is faster than the CRT for N less than 38. However, for large N the sphere decoder becomes prohibitively expensive. The excess fractions estimator is highly computationally complex even for a small number of wavelengths. The computational complexity of the excess fractions estimator depends upon the ratio between the UMR and the smallest wavelength and increases with an increase in this ratio. This complexity can be very high even for three measurement wavelengths if the ratio between the UMR and the smallest wavelength is large.

5.6 Conclusion

From previous chapters we observed that there exists a non trivial relationship between the measurement wavelengths and the accuracy of the least squares range estimator. In this chapter, we provided an algorithm to automatically select an optimised set

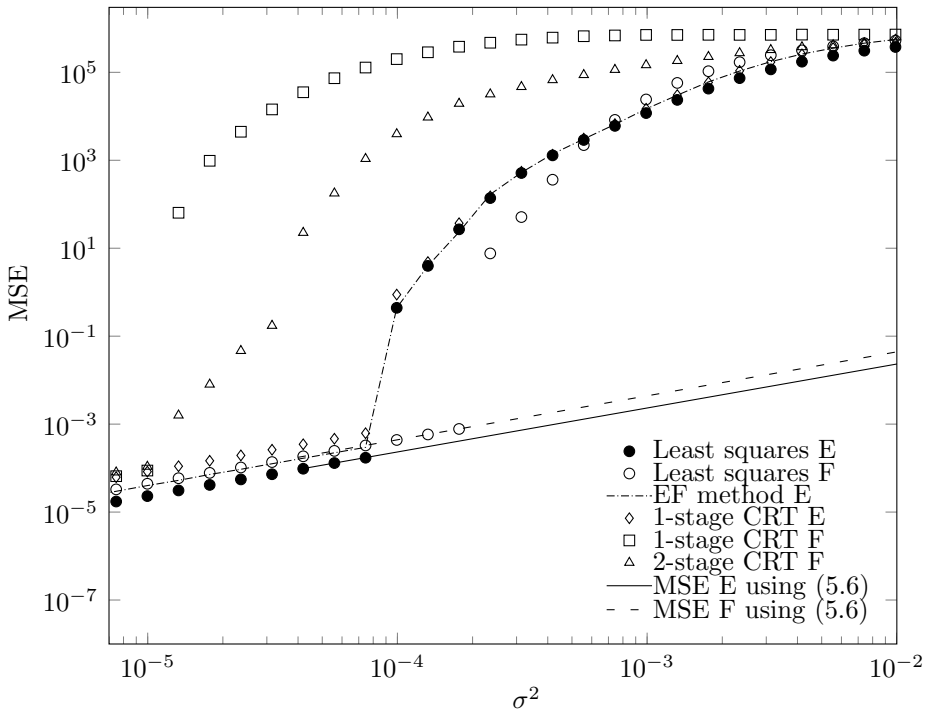

Figure 5.4: Sample mean square error of the least squares range estimator, the excess fraction based range estimator [20] and the range estimator based on the single stage and multi-stage CRT algorithms of Xiao et. al. [31] with $N = 5$ wavelenths.

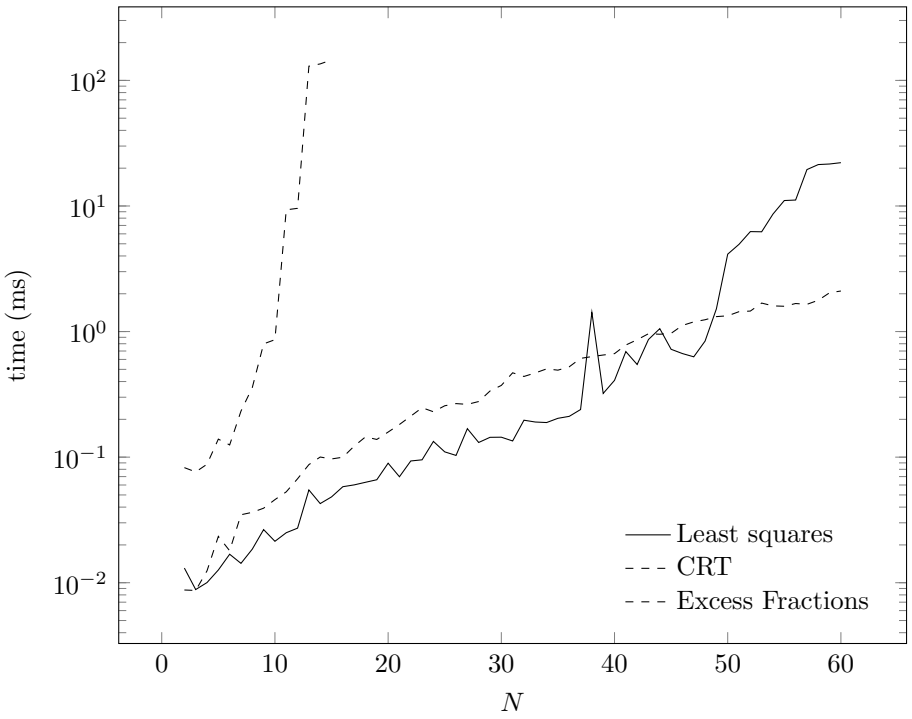

Figure 5.5: Computation time benchmark: Comparison of the least squares estimator, the CRT estimator and the excess fractions estimator.

of wavelengths to maximise the accuracy of the least squares range estimator. This selection procedure is typically subject to practical constraints such as minimum and maximum wavelength (i.e. bandwidth constraints) and constraints on the maximum identifiable range.

The relationship between measurement wavelengths and range estimation accuracy is, however, non trivial and this complicates wavelength selection procedures. In this chapter we first make a key realisation that relates the measurement wavelengths to the determinant of the lattice. This observation helped us to exploit the relationship between the measurement wavelengths and the Voronoi cell of the lattice through an upper bound on the volume of the Voronoi cell.

For the purpose of wavelength selection algorithm, we first defined two approximations for the error of the range estimator in terms of the measurement wavelengths. The first approximates the error in the case that the least squares estimator of the wrapping variables is correct. The second upper bounds the probability that the wrapping variables are correct. Next we formulated an optimisation criterion that aims to minimise the mean square error of the estimator. Based on this optimisation criterion a depth first search algorithm is developed that outputs a set of wavelengths that typically yield smaller mean square error when employed with the least square estimator. Simulations indicate that the wavelengths obtained using this algorithm outperform the existing wavelength selection methods for the excess fractions range estimator and also outperform the CRT based range estimators.

Chapter 6

Conclusion and Future Work

6.1 Introduction

This thesis provided a new insight into the least squares estimation of range using the phase of arrival method. An important realisation made in the existing literature is that the least squares estimator can be efficiently computed by solving a well known integer programming problem, that of computing a closest point in a lattice. General purpose algorithms require a basis for the lattice to compute a closest lattice point. For the least squares estimator an explicit basis construction method was recently provided. This basis construction method is only valid if the measurement wavelengths can be scaled to pair-wise relatively prime integers. This assumption on wavelengths is not practically suitable because using only the wavelengths that can be scaled to pair-wise relatively prime integers may greatly degrade the accuracy of the range estimator. In fact, the accuracy of all the range estimators depends upon the measurement wavelengths. However, the relationship between the measurement wavelengths and the accuracy of these range estimators is not trivial.

The dependence of estimation accuracy upon the measurement wavelengths leads to two important question.

- Whether it is possible to devise a basis construction method that is independent of mutually co-prime restriction on the scaled wavelengths?

- Given a basis construction method that is independent of mutually co-prime restriction on the scaled wavelengths, whether it is possible to select wavelengths that can maximise the accuracy of the least squares range estimator?

These two questions are mainly answered in this thesis.

Chapter 2 presents a brief overview of some introductory concepts from lattice theory. The main concepts related to the Voronoi cell, the nearest lattice point problem, dual lattices, and the properties of lattices generated by intersection with or projection onto a subspace are discussed. These concepts provide a solid foundation for the evaluation of the least squares range estimator in later chapters. This chapter also provides a highlight of other range estimation techniques based on the phase of arrival method. This includes the techniques such as the beat wavelength method, the method of excess fractions, and the CRT method. Wavelength selection methods for the beat wavelength method and the method of excess fractions are also discussed for the completeness of the topic.

Chapter 3 laid the foundation for the realisation of an algorithm to automatically select an optimised set of wavelengths. This chapter first provided the system model that was used throughout the thesis. The problem of range estimation from phase observations at multiple frequencies was described and a least squares estimator of the range was derived. The chapter then described key connection between the least squares estimator and the lattice theory. It was shown that how the least squares estimator can be solved by computing a closest point in a lattice. The main contribution of this chapter was to provide a basis construction method that could be used to compute a closest point in a lattice. The basis construction method provided in this chapter is independent of the restriction that the the scaled wavelengths should be mutually co-prime integers. Moreover, this method is very simple as compared to the existing basis construction method.

Chapter 4 first presents an insight about the correctness of the wrapping variables. The correct wrapping variables are related to the whole number of wavelengths that occur over the range. It is expected that accurate estimators of the wrapping variables are also the accurate estimators of the range. This chapter derives an upper bound on

the phase measurement errors such that if all absolute phase measurement errors are less than this bound, then the least squares range estimator is guaranteed to correctly estimate the wrapping variables and hence the range. An interesting property of the lattice called *inradius* is used to derive this bound. It is observed that this bound is dependent upon the values of the measurement wavelengths. This observation combined with the result from Chapter 3 that a basis can be constructed for a general set of wavelengths lead to a natural question of whether it is possible to select wavelengths that maximise the inradius and hence the accuracy of the least squares range estimator.

Motivated from the results in the previous chapters Chapter 5 addresses the problem of selecting the wavelengths for the least squares estimator to maximise its accuracy. For this purpose the nontrivial relationship between the measurement wavelengths and the Voronoi cell of the lattice was exploited. An important observation was that the Voronoi cell of a lattice can be approximated by a sphere of volume equal to that of the Voronoi cell in the presence of Normally distributed phase noise. The volume of the Voronoi cell is equal to the determinant of the basis matrix. Our basis construction method provided a simple expression to calculate the determinant of the Voronoi cell. It is this simple expression that disclosed the nontrivial relationship between the measurement wavelengths and the Voronoi cell of the lattice. For the purpose of wavelengths selection we consider two approximations. The first approximates the error in the case that the least squares estimator of the wrapping variables is correct. The second upper bounds the probability that the wrapping variables are correct. We formulated an optimisation criterion that aims to minimise the mean square error of the estimator. This optimisation criterion is used to develop a wavelength selection algorithm that provides a set of wavelengths that typically result in smaller mean square error when used with the least square estimator. It is observed from numerical results that this algorithm outputs a set of wavelengths that outperforms the existing wavelength selection methods for the excess fractions range estimator and also outperform the CRT based range estimators.

Bibliography

[1] E. Jacobs and E. W. Ralston, "Ambiguity resolution in interferometry," *IEEE Trans. Aerospace Elec. Systems*, vol. 17, no. 6, pp. 766–780, Nov. 1981.

[2] J. M. M. Anderson, J. M. Anderson, and E. M. Mikhail, *Surveying, theory and practice*, WCB/McGraw-Hill, 1998.

[3] P. J. G. Teunissen, "The LAMBDA method for the GNSS compass," *Artificial Satellites*, vol. 41, no. 3, pp. 89–103, 2006.

[4] P. J. G. Teunissen, "The least-squares ambiguity decorrelation adjustment: a method for fast GPS integer ambiguity estimation," *Journal of Geodesy*, vol. 70, pp. 65–82, 1995.

[5] M. Frank, M. Plaue, H. Rapp, U. Koethe, B. Jhne, and F. A. Hamprecht, "Theoretical and experimental error analysis of continuous-wave time-of-flight range cameras," *Optical Engineering*, vol. 48, no. 1, Jan. 2009.

[6] A. Benedetti, "Methods and systems for geometric phase unwrapping in time of flight systems," United States patent, 0049767 A1, Feb. 2014.

[7] S. D. Chitte, S. Dasgupta, and D. Zhi, "Distance estimation from received signal strength under log-normal shadowing: Bias and variance," *IEEE Signal Process. Letters*, vol. 16, no. 3, pp. 216–218, March 2009.

[8] H.-C. So and L. Lin, "Linear least squares approach for accurate received signal strength based source localization.," *IEEE Trans. Sig. Process.*, vol. 59, no. 8, pp. 4035–4040, 2011.

[9] X. Li and K. Pahlavan, "Super-resolution TOA estimation with diversity for indoor geolocation," *IEEE Trans. Wireless Commun.*, vol. 3, no. 1, pp. 224–234, Jan 2004.

[10] S. Lanzisera, D. Zats, and K.S.J. Pister, "Radio frequency time-of-flight distance measurement for low-cost wireless sensor localization," *IEEE Sensors Journal*, vol. 11, no. 3, pp. 837–845, March 2011.

[11] Fauzia Ahmad, Moeness G. Amin, and Paul D. Zemany, "Performance analysis of dual-frequency CW radars for motion detection and ranging in urban sensing applications," *Proc. SPIE 6547, Radar Sensor Technology XI*, vol. 6547, pp. 65470K–65470K–8, May 2007.

[12] A. Povalac and J. Sebesta, "Phase difference of arrival distance estimation for RFID tags in frequency domain," in *RFID-Technologies and Applications (RFID-TA), 2011 IEEE International Conference on*, Sept 2011, pp. 188–193.

[13] K. Thangarajah, R. Rashizadeh, S. Erfani, and M. Ahmadi, "A hybrid algorithm for range estimation in RFID systems," in *Electronics, Circuits and Systems (ICECS), 2012 19th IEEE International Conference on*, Dec 2012, pp. 921–924.

[14] Burkhard Stiller, Thomas Bocek, Fabio Hecht, Guilherme Machado, Peter Racz, and Martin Waldburger, "Real-Time Kinematic Surveying - Training Guide," Tech. Rep., Trimble Navigation Limited, 01 2003.

[15] D. Grejner-Brzezinska, I. Kashani, P. Wielgosz, D. Smith, P. Spencer, D. Robertson, and G. Mader, "Efficiency and reliability of ambiguity resolution in network-based real-time kinematic GPS," *J. of Surveying Eng.*, vol. 133, no. 2, pp. 56–65, 2007.

[16] D. Odijk, P. Teunissen, and B. Zhang, "Single-frequency integer ambiguity resolution enabled GPS precise point positioning," *J. of Surveying Eng.*, vol. 138, no. 4, pp. 193–202, 2012.

[17] N. I. Fisher, *Statistical analysis of circular data*, Cambridge University Press, 1993.

[18] C. E. Towers, D. P. Towers, and J. D. C. Jones, "Optimum frequency selection in multifrequency interferometry," *Optics Letters*, vol. 28, pp. 887–889, 2003.

[19] Catherine E. Towers, David P. Towers, and Julian D. C. Jones, "Generalized frequency selection in multifrequency interferometry," *Opt. Lett.*, vol. 29, no. 12, pp. 1348–1350, Jun 2004.

[20] Konstantinos Falaggis, David P. Towers, and Catherine E. Towers, "Method of excess fractions with application to absolute distance metrology: theoretical analysis," *Appl. Opt.*, vol. 50, no. 28, pp. 5484–5498, Oct 2011.

[21] K. Falaggis, David P. Towers, and Catherine E. Towers, "Method of excess fractions with application to absolute distance metrology: Wavelength selection and the effects of common error sources," *Appl. Opt.*, vol. 51, no. 27, pp. 6471–6479, Sep 2012.

[22] Konstantinos Falaggis, David P. Towers, and Catherine E. Towers, "Method of excess fractions with application to absolute distance metrology: analytical solution," *Appl. Opt.*, vol. 52, no. 23, pp. 5758–5765, Aug 2013.

[23] Konstantinos Falaggis, David P. Towers, and Catherine E. Towers, "Algebraic solution for phase unwrapping problems in multiwavelength interferometry," *Appl. Opt.*, vol. 53, no. 17, pp. 3737–3747, Jun 2014.

[24] O. Ore, "The general Chinese remainder theorem," *The American Mathematical Monthly*, vol. 59, pp. 365–370, 1952.

[25] O. Goldreich, D. Ron, and M. Sudan, "Chinese remaindering with errors," *IEEE Trans. Inform. Theory*, vol. 46, no. 4, pp. 1330–1338, Jul 2000.

[26] X. G. Xia and K. Liu, "A generalized Chinese Remainder Theorem for residue sets with errors and its application in frequency determination from multiple sensors with low sampling rates," *IEEE Signal Process. Letters*, vol. 12, no. 11, pp. 768–771, Nov 2005.

[27] X. G. Xia and G. Y. Wang, "Phase unwrapping and a robust Chinese Remainder Theorem," *IEEE Signal Process. Letters*, vol. 14, no. 4, pp. 247–250, April 2007.

[28] X. W. Li and X. G. Xia, "A fast robust Chinese Remainder Theorem based phase unwrapping algorithm," *IEEE Signal Process. Letters*, vol. 15, pp. 665–668, 2008.

[29] W. Wang and X. G. Xia, "A closed-form robust Chinese Remainder Theorem and its performance analysis," *IEEE Trans. Sig. Process.*, vol. 58, no. 11, pp. 5655–5666, Nov 2010.

[30] B. Yang, W. Wang, X. G. Xia, and Q. Y. Yin, "Phase detection based range estimation with a dual-band robust Chinese Remainder Theorem," *Science China Information Sciences*, vol. 57, no. 2, pp. 1–9, 2014.

[31] Li Xiao, Xiang-Gen Xia, and Wenjie Wang, "Multi-stage robust Chinese Remainder Theorem," *IEEE Trans. Sig. Process.*, vol. 62, no. 18, pp. 4772–4785, Sept 2014.

[32] A. Hassibi and S. P. Boyd, "Integer parameter estimation in linear models with applications to GPS," *IEEE Trans. Sig. Process.*, vol. 46, no. 11, pp. 2938–2952, Nov 1998.

[33] W. Li, X. Wang, X. Wang, and B. Moran, "Distance estimation using wrapped phase measurements in noise," *IEEE Trans. Sig. Process.*, vol. 61, no. 7, pp. 1676–1688, 2013.

[34] A. Akhlaq, R. McKilliam, and R. Subramanian, "Basis construction for range estimation by phase unwrapping," *Signal Processing Letters, IEEE*, vol. PP, no. 99, pp. 1–1, 2015.

[35] E. Agrell, T. Eriksson, A. Vardy, and K. Zeger, "Closest point search in lattices," *IEEE Trans. Inform. Theory*, vol. 48, no. 8, pp. 2201–2214, Aug. 2002.

[36] J. H. Conway and N. J. A. Sloane, *Sphere packings, lattices and groups*, Springer, New York, 3rd edition, 1998.

[37] J. Martinet, *Perfect lattices in Euclidean spaces*, Springer, 2003.

[38] R. G. McKilliam, W. D. Smith, and I. V. L. Clarkson, "Linear-time nearest point algorithms for Coxeter lattices," *IEEE Trans. Inform. Theory*, vol. 56, no. 3, pp. 1015–1022, Mar. 2010.

[39] D. Micciancio and P. Voulgaris, "A deterministic single exponential time algorithm for most lattice problems based on Voronoi cell computations," *SIAM Journal on Computing*, vol. 42, no. 3, pp. 1364–1391, 2013.

[40] R. McKilliam, A. Grant, and I. Clarkson, "Finding a closest point in a lattice of Voronoi's first kind," *SIAM Journal on Discrete Mathematics*, vol. 28, no. 3, pp. 1405–1422, 2014.

[41] J. H. Conway and N. J. A. Sloane, "A fast encoding method for lattice codes and quantizers," *IEEE Trans. Inform. Theory*, vol. 29, no. 6, pp. 820–824, Nov 1983.

[42] U. Erez and R. Zamir, "Achieving $1/2\log(1+SNR)$ on the AWGN channel with lattice encoding and decoding," *IEEE Trans. Inform. Theory*, vol. 50, no. 10, pp. 2293–2314, Oct. 2004.

[43] D. Wubben, D. Seethaler, J. Jalden, and G. Matz, "Lattice reduction," *IEEE Signal Processing Magazine*, vol. 28, no. 3, pp. 70–91, 2011.

[44] R. G. McKilliam, B. G. Quinn, and I. V. L. Clarkson, "Direction estimation by minimum squared arc length," *IEEE Trans. Sig. Process.*, vol. 60, no. 5, pp. 2115–2124, May 2012.

[45] R. G. McKilliam, B. G. Quinn, I. V. L. Clarkson, and B. Moran, "Frequency estimation by phase unwrapping," *IEEE Trans. Sig. Process.*, vol. 58, no. 6, pp. 2953–2963, June 2010.

[46] I. V. L. Clarkson, "Approximate maximum-likelihood period estimation from sparse, noisy timing data," *IEEE Trans. Sig. Process.*, vol. 56, no. 5, pp. 1779–1787, May 2008.

[47] R. G. McKilliam and I. V. L. Clarkson, "Identifiability and aliasing in polynomial-phase signals," *IEEE Trans. Sig. Process.*, vol. 57, no. 11, pp. 4554–4557, Nov. 2009.

[48] R. G. McKilliam, B. G. Quinn, I. V. L. Clarkson, B. Moran, and B. N. Vellambi, "Polynomial phase estimation by least squares phase unwrapping," *IEEE Transactions on Signal Processing*, vol. 62, no. 8, pp. 1962–1975, April 2014.

[49] R.G. McKilliam, I.V.L. Clarkson, and B.G. Quinn, "Fast sparse period estimation," *IEEE Signal Processing Letters*, vol. 22, no. 1, pp. 62–66, Jan 2015.

[50] W. Li, X. Wang, X. Wang, and B. Moran, "Resolving phase measurement ambiguity in presence of coloured noise," *Electronics Letters*, vol. 49, no. 18, pp. 1188–1190, August 2013.

[51] D. Micciancio, "The hardness of the closest vector problem with preprocessing," *IEEE Trans. Inform. Theory*, vol. 47, no. 3, pp. 1212–1215, 2001.

[52] I. Dinur, G. Kindler, and S. Safras, "Approximating CVP to within almost-polynomial factors in NP-hard," *Combinatorica*, vol. 23, pp. 205–243, 2003.

[53] J. Jalden and B. Ottersten, "On the complexity of sphere decoding in digital communications," *IEEE Trans. Sig. Process.*, vol. 53, no. 4, pp. 1474–1484, April 2005.

[54] J. H. Conway and N. J. A. Sloane, "Fast quantizing and decoding and algorithms for lattice quantizers and codes," *IEEE Trans. Inform. Theory*, vol. 28, no. 2, pp. 227–232, Mar. 1982.

[55] J. H. Conway and N. J. A. Sloane, "Soft decoding techniques for codes and lattices, including the Golay code and the Leech lattice," *IEEE Trans. Inform. Theory*, vol. 32, no. 1, pp. 41–50, Jan. 1986.

[56] Yuke Wang, "New Chinese remainder theorems," *Conference Record of the Thirty-Second Asilomar Conference on Signals, Systems and Computers*, vol. 1, pp. 165–171 vol.1, Nov 1998.

[57] G. Wang, X. G. Xia, and V. C. Chen, "Detection, location, and imaging of fast moving targets using multifrequency antenna array SAR," *IEEE Trans. Aerospace Elec. Systems*, vol. 40, no. 1, pp. 345–355, Jan 2004.

[58] X. Li, H. Liang, and X. G. Xia, "A robust Chinese Remainder Theorem with its applications in frequency estimation from undersampled waveforms," *IEEE Trans. Sig. Process.*, vol. 57, no. 11, pp. 4314–4322, Nov 2009.

[59] X. Li and X. G. Xia, "Location and imaging of elevated moving target using multi-frequency velocity SAR with cross-track interferometry," *IEEE Trans. Aerospace Elec. Systems*, vol. 47, no. 2, pp. 1203–1212, April 2011.

[60] L. Babai, "On Lovász lattice reduction and the nearest lattice point problem," *Combinatorica*, vol. 6, pp. 1–13, 1986.

[61] K. V. Mardia and P. Jupp, *Directional Statistics*, John Wiley & Sons, 2nd edition, 2000.

[62] R. G. McKilliam, *Lattice theory, circular statistics and polynomial phase signals*, Ph.D. thesis, University of Queensland, Australia, December 2010.

[63] S. A. Tretter, "Estimating the frequency of a noisy sinusoid by linear regression," *IEEE Trans. Inform. Theory*, vol. 31, no. 6, pp. 832–835, November 1985.

[64] I. Vrana, "Optimum statistical estimates in conditions of ambiguity," *IEEE Trans. Inform. Theory*, vol. 39, no. 3, pp. 1023–1030, May 1993.

[65] B. G. Quinn, "Phase-only information loss," *Proc. Internat. Conf. Acoust. Spe. Sig. Process.*, pp. 3982–3985, Mar. 2010.

[66] Arash Hassibi and Stephen Boyd, "Integer parameter estimation in linear models with applications to GPS," *ieeetsp*, vol. 46, no. 11, pp. 2938–2952, Nov. 1998.

[67] M. Pohst, "A modification of the LLL reduction algorithm," *J. Symbolic Computation*, , no. 4, pp. 123–127, 1987.

[68] H. Cohen, *A course in computational algebraic number theory*, Springer Verlag, 1993.

[69] A. Pollok A. Akhlaq, R. G. McKilliam, "Robustness of the least squares range estimator," accepted to the Australian Communications Theory Workshop (AusCTW), 2016.